1-2011

How do neurons work together? Lessons from auditory cortex

Kenneth D. Harris
Rutgers University, kenneth.harris@ucl.ac.uk

Peter Bartho
Rutgers University

Paul Chadderton
Rutgers University

Carina Curto
University of Nebraska - Lincoln, ccurto2@math.unl.edu

Jaime de la Rocha
Rutgers University

See next page for additional authors

Published in final edited form as:
Hear Res. 2011 January ; 271(1-2): 37–53. doi:10.1016/j.heares.2010.06.006.

How do neurons work together? Lessons from auditory cortex

Kenneth D. Harris[1,2,3], **Peter Bartho**[1,4], **Paul Chadderton**[1,5], **Carina Curto**[1,6], **Jaime de la Rocha**[1], **Liad Hollender**[1], **Vladimir Itskov**[1,6], **Artur Luczak**[1,7], **Stephan L. Marguet**[1], **Alfonso Renart**[1], and **Shuzo Sakata**[1]

[1] Center for Molecular and Behavioral Neuroscience, Rutgers University, 197 University Avenue, Newark NJ 07102, USA

[2] Smilow Neuroscience Program and Department of Otolaryngology, New York University Medical School, 530 First Avenue, New York, NY 10016, USA

[3] Departments of Bioengineering, Electrical and Electronic Engineering, Imperial College London, London SW7 2AZ, UK

[4] Institute of Experimental Medicine, Hungarian Academy of Sciences, Budapest 1083, Hungary

[5] UCL Ear Institute, London WC1X 8EE, UK

[6] Department of Mathematics, University of Nebraska-Lincoln, Lincoln, NE 68588-0130, USA

[7] Canadian Centre for Behavioural Neuroscience, Dept. of Neuroscience, University of Lethbridge, 4401 University Drive, Lethbridge, AB, T1K 3M4, Canada

Abstract

Recordings of single neurons have yielded great insights into the way acoustic stimuli are represented in auditory cortex. However, any one neuron functions as part of a population whose combined activity underlies cortical information processing. Here we review some results obtained by recording simultaneously from auditory cortical populations and individual morphologically identified neurons, in urethane-anesthetized and unanesthetized passively listening rats. Auditory cortical populations produced structured activity patterns both in response to acoustic stimuli, and spontaneously without sensory input. Population spike time patterns were broadly conserved across multiple sensory stimuli and spontaneous events, exhibiting a generally conserved sequential organization lasting approximately 100ms. Both spontaneous and evoked events exhibited sparse, spatially localized activity in layer 2/3 pyramidal cells, and densely distributed activity in larger layer 5 pyramidal cells and putative interneurons. Laminar propagation differed however, with spontaneous activity spreading upward from deep layers and slowly across columns, but sensory responses initiating in presumptive thalamorecipient layers, spreading rapidly across columns. In both unanesthetized and urethanized rats, global activity fluctuated between “desynchronized” state characterized by low amplitude, high-frequency local field potentials and a “synchronized” state of larger, lower-frequency waves. Computational studies suggested that responses could be predicted by a simple dynamical system model fitted to the spontaneous activity immediately preceding stimulus presentation. Fitting this model to the data yielded a nonlinear self-exciting system model in synchronized states and an approximately linear system in desynchronized states. We comment on the significance of these results for auditory cortical processing of acoustic and non-acoustic information.

Correspondence to kenneth.harris@imperial.ac.uk.

Introduction

Experimental studies of neural activity *in vivo* have historically focused on the spiking of single neurons. In the auditory cortex, single-unit recordings have revealed a great deal about how the firing of individual neurons is modulated by acoustic stimuli. However, any one neuron functions only as part of a much larger population whose combined activity underlies an animal's processing of information. Characterizing the structure of neuronal population activity, and its relationship to sensory stimuli, is a key step toward understanding how information is processed in auditory cortex. Over the last decade or so, technological advances such as the development of tetrodes, silicon microelectrode arrays, and spike-sorting techniques have allowed for recording the activity of up to hundreds of neurons simultaneously *in vivo*. Although these techniques were first developed for use in the hippocampus (Csicsvari et al., 2003; Harris et al., 2000; McNaughton et al., 1983; Recce et al., 1989; Schmitzer-Torbert et al., 2005), they can be used in many other brain structures (Bartho et al., 2004; Berke et al., 2004; Felsen et al., 2008; Gray et al., 1995; Luczak et al., 2007; Ranade et al., 2009). This article reviews some recent research using microelectrode arrays to study the activity of neural populations within auditory cortex. We will discuss: the structure of population spiking activity in auditory cortex; the relation of sound-evoked to spontaneous activity; the organization of this activity across cortical layers; and its modulation by brain state.

Spontaneous activity in auditory cortex

A classical view of sensory cortex is that neural activity is driven by external stimuli. Although neurons in sensory cortices do fire action potentials without stimuli (e.g. in silence or darkness for auditory and visual cortices, respectively), this is usually considered “baseline” activity. Analysis of this spontaneous activity usually consists simply of calculating the “baseline firing rate” for each neuron (i.e. its mean rate prior to stimulus presentation), which is then used as a comparison point for sensory responses. Based on this knowledge alone, one might imagine that in the absence of sensory stimuli, all neurons fired tonically at baseline rate, corresponding to globally unstructured population activity. This, however, is not always the case. While cortical background activity can be unstructured (even in recurrent neural circuits with strong and dense shared inputs; see section on brain states below), it can also display highly structured population activity even in the absence of sensory stimuli (Fig. 1; Renart et al 2010).

The structure of cortical population activity is intimately related to a well studied neural signal, the local field potential (LFP). LFP reflects synaptic currents rather than spiking activity, and the LFP at any laminar position reflects a complex summation of currents across produced by multiple inputs onto cells of all layers (Einevoll et al., 2007; Kandel et al., 1997; Mitzdorf, 1985; C. Schroeder, this issue). Nevertheless, there is a robust correlation between the LFP and local population activity (Katzner et al., 2009). In general, deep layer LFP anticorrelates with the instantaneous firing rate of the local population, with negative LFP deflections at times of increased firing rate (Fig 1). This phenomenon occurs in multiple sensory cortices, and LFP also correlates negatively and robustly with neuronal membrane potentials (Poulet et al., 2008). Cortical LFP, and its relation to behaviour, has been intensely studied for decades (see e.g. John et al., 1973; Vanderwolf, 2003). Thus, even though the ability to record neural populations is relatively recent, earlier studies of LFP provide important, if indirect, information about the structure of population activity.

The structure of spontaneous cortical activity varies with brain state, which itself varies according to behavioural and cognitive conditions (Steriade et al., 1993a; Steriade et al.,

2001; Vanderwolf, 2003). Spontaneous activity is often dominated by slow (~<4Hz) fluctuations in global activity levels, with the firing rates of simultaneously recorded neurons increasing and decreasing together in a manner that correlates with ongoing slow LFP oscillations (as illustrated in Fig. 1). These global fluctuations are often characterized by transient periods in which almost none of the recorded neurons fire, typically accompanied by dome-shaped positive deflections in the deep-layer LFP and hyperpolarization of membrane potentials. The length of these periods varies with brain state, ranging from several seconds under certain anesthetic conditions (Steriade et al., 1993b), to as short as tens of milliseconds in awake quiescent animals (Luczak et al., 2009; Luczak et al., 2007; Poulet et al., 2008). Here we use the terms “downstate” to describe such periods of network inactivity, and “upstate” for the alternative periods, where the network is spontaneously active (but note that some authors reserve these terms for the long periods of hyperpolarization and depolarization seen in anesthesia and sleep).

The vocabulary of neuronal populations

In principle, the number of spatiotemporal patterns that could be produced by even a small number of neurons is astronomical. How much of this potential capacity is actually realized? To investigate this, Luczak et al (2009) analyzed the structure of the initial (100ms) component of auditory cortical responses to tones and natural sounds, and spontaneous upstates.

Constraints on spike timing are preserved across spontaneous and sensory-evoked conditions

To investigate the constraints on the spike patterns expressible by a neuronal population, we recorded simultaneously from 40-100 neurons in layer 5 of rat auditory cortex using silicon microelectrodes. Experiments were conducted in urethane-anesthetized and unanesthetized passively listening rats. In response to tone stimuli, individual neurons showed diverse but consistent temporal firing profiles, indicating that tone presentation causes a stereotyped spatiotemporal activity pattern in the recorded population (Fig. 2). To test whether different sensory stimuli induce similar sequential patterns at onset, we also analyzed the response of the same population to multiple natural sound stimuli (insect vocalizations). Examination of individual neuron and population responses revealed timing patterns homologous to those evoked by tone presentation, suggesting that responses to natural sounds are constrained to a similar sequential ordering (Luczak et al. 2009). Spontaneous patterns also showed a similar sequential structure as sensory responses. Individual neurons showed similar temporal relationships of their spiking activity to upstate onsets as they did to sensory stimuli, revealing a similar sequential structure at the population level (Fig 3).

To statistically verify these observations, we computed a measure μ_{cc} of each neuron's position in a firing sequence, defined as the center of mass of its cross-correlogram with the summed activity of all other neurons, computed in the first 100ms after the onset of each event type (Luczak et al., 2009). Values of μ_{cc} were strongly correlated between stimulus classes, demonstrating that the order of neural firing is consistent between sensory stimuli, as well as spontaneous events ($R_{\text{ureth: ton-nat}} = 0.69\pm0.21$, N=5 rats; $R_{\text{ureth: spont-ton}} = 0.6\pm0.14$; $R_{\text{ureth: spont-nat}} = 0.57\pm0.18$; $R_{\text{unanesth: spont-ton}} = 0.53\pm0.17$; numbers give mean ±s.d.; $p<0.001$ for each dataset; Luczak et al. 2009;). We thus concluded that the possible sequential firing orders that a given cortical population may exhibit – either spontaneously or in response to sensory stimuli – are highly constrained. Similar relationships between constraints on spontaneous and evoked firing sequences have also been observed in somatosensory and visual cortices (Jermakowicz et al., 2009; Luczak et al., 2009)

At first this result might appear to contradict previous findings obtained from single-cell recordings, which have demonstrated that neuronal latencies may vary between stimuli, typically being shortest for a neuron's preferred stimulus (Heil, 2004; Oram et al., 2002). We also observed this phenomenon; however, the variability of latencies across stimuli for a single neuron was typically much smaller than the variability of latencies across neurons for a single stimulus (Luczak et al. 2009), causing little perturbation of the overall sequential structure. Although temporal response profiles would be expected to vary between cortical areas and layers (see below), the diversity we observed did not simply reflect this, as diverse temporal profiles were observed even amongst neighboring neurons recorded from the same tetrode (Luczak et al., 2009; Luczak et al., 2007). Heterogeneity of neighboring A1 neurons has also been reported by recent optical imaging studies of frequency tuning (Bandyopadhyay et al., 2010; Rothschild et al., 2010). Thus, even though auditory cortex has large scale organization in the form of tonotopy and inter-area differences, presentation of even a pure tone sets off a complex dynamic pattern of spiking activity spanning large regions of auditory cortex, whose spatial and temporal structure determined by local circuit properties as well as tonotopy and areal structure.

The finding that auditory cortical neurons show complex temporal dynamics, including delayed onsets and sustained firing during tone presentation, is consistent with reports of previous single-cell recordings in awake, ketamine-, halothane- or barbiturate-anesthetized subjects (Moshitch et al., 2006; Sally et al., 1988; Volkov et al., 1991; Wang et al., 2005) but contrasts with other reports using barbiturates or ketamine-xylazine (e.g. deCharms et al., 1996; DeWeese et al., 2003), which have suggested precisely timed firing of sometimes only one spike at onset, but not sustained rate changes. We have not conducted a systematic analysis of the effects of different anesthetics on temporal patterns responses. However our results, together with previous studies, suggest that while some anesthetic conditions might suppress sustained responses and complex temporal response patterns, the absence of auditory cortical sustained responses is not a consequence of anesthesia *per se*, but only of certain anesthetic/stimulus conditions.

Constraints on firing rate patterns are preserved across spontaneous and sensory-evoked conditions

We next asked whether the possible combinations of firing rates expressible by the population are also subject to common constraints across various stimuli and spontaneous events. For this analysis we discarded temporal information, and summarized each population pattern by a vector containing the firing rates of each recorded neuron during the first 100 milliseconds after stimulus or upstate onset.

To gain insight into the nature of constraints on firing rates, we initially focused on cell pairs. Figure 4A illustrates, for one pair of cells, the number of spikes fired in individual upstates (black dots), responses to a representative tone (green), and responses to a natural sound (red). The region occupied by upstate spike counts has a triangular shape, suggesting a constraint on possible spike count combinations: if neuron 2 fired in any given upstate, neuron 1 almost always fired also. The regions occupied by the responses to the two stimuli differed, but both fell within the region outlined by the set of spontaneous events. Figure 4B shows, in outline view, the regions occupied by responses to the two stimuli and spontaneous upstates, and a set of vectors in which spike count correlations had been destroyed by shuffling (spontaneous spike counts were shuffled for each neuron separately, preserving each cell's firing rate distribution but enforcing independence between neurons). Part of the realm of shuffled responses (marked in gray) is not occupied by either spontaneous or evoked responses, indicating that these spiking combinations are not produced by the circuit.

We next asked whether a similar phenomenon occurs at the level of the full spike count vectors. Visualization of high-dimensional data requires techniques to map this data into two dimensions. We used multidimensional scaling (Kruskal et al., 1978), a nonlinear method whereby points which are close in the original high-dimensional space will also be placed close together in the 2D projection (Figures 4C and 4D) (see also Gerstein et al., 1985). It can be seen that each stimulus produces response vectors that occupy a specific region within the realm outlined by spontaneous activity, which is itself contained in the realm outlined by shuffled patterns. To quantitatively verify this, we compared the distance from each evoked event to its nearest neighbour in the set of spontaneous events, with the distance to its nearest neighbour in the set of shuffled spontaneous events (all distances computed in the full space of spike count vectors, not the 2d projection). The set of shuffled events was created by randomly reassigning neuronal responses between spontaneous events, and so represents the set of firing patterns the population could produce if there were no relationships between the spike counts of different neurons. This space contains the set of original unshuffled events, but is larger, and the same number of events therefore fills it with a lower density. Thus, if sensory responses occupy the same subspace as spontaneous events, the distance from a sensory response to its nearest neighbour in the shuffled events should be larger than to its nearest neighbour in the set of unshuffled events. Statistical tests confirmed that this was indeed the case (Figures 4E-4G; Luczak et al 2009). Thus, spike count vectors accompanying spontaneous events occupy only a small region of the space of possible rate vectors, with the responses to individual sensory stimuli lying within this "allowed region."

In summary, for the initial period of sensory responses, both the combinations of cells that can fire and the possible orders in which they can fire are subject to constraints that are preserved across stimuli. Similar constraints also apply to the population patterns occurring at the start of spontaneous upstates. This result raises a question: are spontaneous and sensory-evoked patterns so similar as to be identical (and thus indistinguishable to downstream neurons)? The above findings were all based on recordings from a single layer, cortical layer 5; as we will see later, there are differences in how spontaneous and evoked activity is organized across layers.

Vector evolution of tone responses

Even though the spatiotemporal responses of neuronal populations are subject to conserved constraints, responses to different stimuli are not identical. To investigate how population responses differ between tone stimuli, Bartho et al (2009) used an approach based on the *firing rate vector* (Laurent, 2002; Stopfer et al., 2003), a representation **f** of the mean rate across trials of a population of N cells, as a point in an N-dimensional space. Considering the dependence of this vector on time, one obtains a trajectory **f**(t) that characterizes the dynamics of the population rate – that is, a description of how it evolves during stimulus presentation. Although this approach cannot capture trial-to-trial variability and noise correlation, it provides information about how mean responses vary between stimuli, and allows the use of geometrical concepts that can help to understand the operation of neural populations. Furthermore, because the method characterizes the mean response to a stimulus rather than inter-neuronal relationships on individual trials, it allows analysis of very large "virtual populations" obtained by pooling cells recorded in multiple experiments (see (Harris, 2005) for further discussion of real vs. virtual populations).

Figure 5A1 shows trajectories evoked by 1 second long pure tones, viewed using principal component analysis (PCA) to project onto the two dimensions accounting for the maximum fraction of total variance. The most striking feature of this plot is the similarity of trajectories for different tone stimuli. Onset responses were seen in this projection as a

circular trajectory that was largely independent of tone frequency. Sustained responses were barely distinguishable from baseline firing in this projection, and offset responses again showed circular profiles, broadly similar between tone frequencies, but different to those seen at onset. Cells contributing the most to this projection had prominent onset and offset responses, but barely any sustained responses (Fig 5A2). The similarity of trajectories produced by different tone frequencies likely results from the conserved constraints described earlier. Figure 5B1 shows trajectories projected onto two dimensions using a different method, multiple discriminant analysis, to select the projection optimizing the separation of sustained firing rates. In this projection sustained responses were clearly distinguishable from baseline and from each other. The PCA and MDA projections provide two views of the same underlying reality: although similarities between responses to different stimuli dominate the PCA projections (which pick the directions of maximum variance, without reference to the underlying stimuli), MDA reveals that information about stimuli is indeed present, but must be extracted using an appropriately chosen projection.

The visualization analysis suggested that presentation of tone stimuli caused rate vectors to rotate in a manner broadly similar across tones, leading to fixed points which differ from the onset trajectories of the same stimulus, and are also distinct between different stimuli. In principle, rotation is not the only way that rate vectors could evolve during sustained stimuli: if the dynamics of tone responses consisted only of firing rate adaptation, and the firing rate of all neurons adapted at the same rate, vectors would shrink linearly throughout the tone time course, but not rotate (Fig. 6A). To characterize population vector rotation, we performed an analysis of the angles between rate vectors. For a particular reference vector, observed in response to a stimulus s_0 at post-stimulus time t_0, the angle between the reference vector $\mathbf{f}_{s_0}(t_0)$ and all other vectors $\mathbf{f}_s(t)$ was computed, after subtraction of the baseline firing rate vector $\bar{\mathbf{f}}$. Figure 6B shows four examples of this analysis. Responses to different frequencies, but at the same time (e.g. onset vs. onset) are closer in angle than responses to the same frequency at different times. Statistical analysis confirmed that the transition between onset and sustained responses consists of a nonlinear population vector rotation, and that the angular difference between responses to the same tone at different times exceeds the difference between different tones at the same time (Bartho et al., 2009). This is consistent with the results of the previous section: if the set of neurons that can fire at early times differs to the set that can fire at late times, one would expect that population vectors corresponding to different post-stimulus times could not be similar, even for the same tone frequency.

Laminar organization of cortical population activity

The six-layered structure of the neocortex is one of the most prominent features of the mammalian brain. Although investigations of the “circuit diagram” of auditory cortex are still ongoing (Barbour et al., 2008; Oswald et al., 2008; Oswald et al., 2009), auditory cortical laminar organization appears to follow a broadly similar pattern to other sensory areas (Linden et al., 2003), despite some differences such as the absence of spiny stellate cells in layer (L)4 (Smith et al., 2001). Primary thalamic afferents in auditory cortex show a bias toward lower L3 and L4, and the L5/6 border (Kimura et al., 2003; Romanski et al., 1993; Winer et al., 2007). The thalamus, however, is not the only source of input to auditory cortex; another major input to primary auditory cortex consists of “feedback” projections from higher order cortical regions, which project heavily to deep layers (Felleman et al., 1991; Rouiller et al., 1991).

To study the laminar organization of auditory cortical activity, Sakata and Harris (2009) used large-scale extracellular recordings using silicon probes and juxtacellular recordings with neurobiotin-filled pipettes (Pinault, 1996), in urethane-anesthetized and unanesthetized

rats. The juxtacellular electrodes yielded recordings of single morphologically reconstructed neurons, whose activity could be analyzed in the context of a larger population of unreconstructed neurons recorded simultaneously with the silicon probes. Although the juxtacellular recordings did not yield a large enough number of morphologically identified interneurons (INs) to perform statistical analyses, putative INs could be identified in the silicon probe recordings by spike waveform.

Similarities in the laminar sparseness profile of sensory-evoked and spontaneous activity

One striking similarity between auditory-evoked and spontaneous activity concerned the sparseness of activity of different cell types. As shown in Figures 7A-B, L2/3 pyramidal cells (PCs) exhibited highly selective responses to stimuli, in both the spectral and temporal domains, while L5 thick PCs (L5 tPCs) were broadly tuned to both stimuli. L4 PCs and L5 slender PCs (L5 sPCs) were intermediate between two classes. Intriguingly, L6 PCs showed strikingly different response profiles than other classes, typically without clear frequency-tuned responses, but sometimes responding to tones and clicks after a ~200ms delay. The tuning of putative INs also differed from that of PCs, with superficial putative INs showing broader tuning, more similar to deep PCs than to superficial PCs (Figure 7C). We confirmed this impression with a “response probability” measure, defined as the probability that a neuron would fire at least one spike in response to any given stimulus presentation (Figure 7E). L2/3 and L6 PCs showed sparsest activity (i.e. lowest response probabilities), and L5 tPCs showed the densest activity (i.e. highest response probabilities). Putative INs of both superficial and deep layers showed response probability similar to that of deep PCs rather than superficial PCs. Thus, we found clear laminar and cell-type-dependent differences in auditory responses, with sparse activity in L2/3 PCs, and denser activity in larger L5 PCs and putative INs. These results are generally consistent with other recordings in multiple sensory cortices, that have identified neuronal classes using multiple methods (Brecht et al., 2003;Brecht, 2007;de Kock et al., 2007;Sohya et al., 2007;Swadlow, 1988;Swadlow, 1989;Swadlow, 1994;Turner et al., 2005;Wallace and Palmer, 2008;Wu et al., 2008)(Zhou et al., 2010) (but see also Hromadka et al., 2008).

We next asked whether similar patterns of sparseness also apply to spontaneous activity patterns. We began by examining patterns of multi-unit activity (MUA), recorded with linear multisite electrodes (Figure 7D). Some, but not all upstates visible in deep layers were accompanied by activity in the immediately overlying superficial layers. To investigate the participation of different identified cell classes in upstates, we again used a response probability measure, here defined as the probability a cell would fire at least one spike in any given upstate (Figure 7F). A similar pattern of sparseness was seen as for auditory responses, with L2/3 and L6 PCs showing the lowest response probability, and L5 tPCs the highest. Response probability was correlated on a cell-to-cell basis between spontaneous and auditory-evoked activity (Figure 7G), suggesting that consistent variations in sparseness both between and within cell classes were preserved in spontaneous and evoked activity.

The results described above focused on the properties of individual neurons, but not the organization of activity across multiple columns. For example, sparse firing of superficial PCs could reflect either activation of localized clusters in discrete points on the cortical surface, or sparse activation of neurons distributed over a wide area. Because primary auditory cortex is tonotopically organized, we expected that for tone responses, activity should be spatially localized; furthermore, it has been reported that both evoked and spontaneous auditory cortical correlations increase with similarity of receptive fields (Brosch et al., 1999; Eggermont, 2006). We addressed this issue using spike-sorted extracellular population activity recorded from multi-shank silicon probes. Visual

examination of rasters suggested spiking activity in superficial layers to be locally clustered, for upstates as well as responses to tones and clicks (Sakata et al., 2009); in deep layers activity was more broadly spread for all types of activity. The structure of neuronal correlations bore this out: in superficial layers, correlations were stronger for local than distal pairs, while in deep layers, there were only subtle differences between local and distal correlations. We note that this picture of superficial layer activity is further supported by a recent *in vivo* calcium imaging study (Rothschild et al., 2010).

Differences in the propagation of sensory-evoked and spontaneous activity

The above analyses showed that the pattern of sparseness across cortical cell classes was similar between evoked and spontaneous activity. However, we also observed a clear difference between these two types of events in the propagation of activity between layers and columns (Figure 8).

Figure 8A shows examples of laminar MUA traces during successive evoked and spontaneous spiking events. At the onset of auditory responses, activity originated in the upper middle and a part of deep layers. These layers correspond to the presumptive locations of strongest inputs from primary thalamus (Kimura et al., 2003), and also match the locations of early current sinks revealed by current source density (Kaur et al., 2005; Sakata et al., 2009; Szymanski et al., 2009), as well as unit recordings in other species such as cats (Atencio et al., 2010) and guinea pigs (Wallace et al., 2008). Activity at upstate onsets, however, was first seen in the deep layers and spread upward, more closely resembling the propagation of spontaneous upstates in *in vitro* slice models (Sanchez-Vives et al., 2000) than the propagation of sensory responses. We quantitatively confirmed the difference between these patterns with a “peak latency” measure, defined as median MUA spike time in a 50ms window after event onset, as a function of putative laminar location (Figure 8B). Similar results have recently been reported in multiple areas of cat cortex (Chauvette et al., 2010).

To investigate the spatial spread of activity across both cortical layers and columns, we next employed a different experimental approach (Figure 8C), in which multisite electrodes were inserted parallel to the layers of auditory cortex. Figures 8D and E show examples of MUA traces recorded with this approach, for upstates and evoked responses, respectively. Activity was more spatially localized in superficial than in deep layers, which is consistent with the cell-type-dependent activation across layers (Figure 7).

However, the speed with which activity spread across recording sites was on average faster for evoked events than for upstates, consistent with the tendency for the latter to sometimes propagate as “traveling waves” (Luczak et al., 2007; Petersen et al., 2003) (Figure 8F). These laminar structures of population activity held under both anesthetized and unanesthetized conditions (Sakata et al., 2009). Thus, the propagation of spontaneous and evoked activity differed, with spontaneous activity spreading upward from deep layers and slowly across columns, but sensory responses initiating in presumptive thalamorecipient layers, spreading rapidly across columns (Figure 8G).

Brain states

The structure of cortical spontaneous activity is not constant, but varies from moment to moment according to the overall state of the cortex. A classical view holds that cortical state is a function of the sleep cycle: during waking or rapid eye movement sleep, the cortex operates in the *desynchronized* (or *activated*)state, characterized by low-amplitude, high-frequency LFP patterns; during slow-wave sleep, the cortex operates in the *synchronized* (or

inactivated) state, characterized by larger, lower-frequency LFP fluctuations corresponding to an alternation of upstates of generalized activity and downstates of network silence.

In addition to the major changes that occur with the sleep cycle, there are gradations in brain state during waking. In quietly resting rodents, cortical activity shows an intermediate pattern in which downstates of reduced length and depth are observed (Fig. 1; Luczak et al., 2009;Luczak et al., 2007;Petersen et al., 2003;Poulet et al., 2008). Brain state is controlled by many factors including the activity of ascending neuromodulatory systems, that vary not just with the sleep-wake cycle but also with behavioral and cognitive variables, that are also associated with changes in LFP and EEG power spectra, and in the size of spiking correlations and global activity fluctuations (Buzsaki et al., 1988;Cohen et al., 2009;Fries et al., 2001;Mitchell et al., 2009;Pesaran et al., 2002;Poulet et al., 2008;Wiest et al., 2003). High-frequency LFP power and synchrony increase, while low-frequency power and correlations decrease in conditions of attention, effects that can occur even locally within receptive fields in the visual system (Cohen et al., 2009;Fries et al., 2001;Mitchell et al., 2009). High-frequency LFP power is also positively correlated with the fMRI BOLD signal (Logothetis et al., 2001), suggesting that levels of desynchronization may vary across the cortex in a task-dependent manner, similarly to the BOLD signal itself. The relationship between spontaneous activity in sensory cortices, and ongoing cognition and behaviour, is likely to in turn affect the cortical response to incoming sensory stimuli (Haider et al., 2007;Hasenstaub et al., 2007;Lakatos et al., 2007). Spontaneous neural activity has been suggested to underlie processes such as mental imagery during waking (Kosslyn et al., 2001;Kraemer et al., 2005;Kreiman et al., 2000), and the reactivation and consolidation of memories during sleep (Buzsaki, 1989;Hoffman et al., 2002;Hoffman et al., 2007).

Under anesthesia, the cortex usually operates in the synchronized state. However, under urethane, desynchronized periods may occur spontaneously, be induced by a tail pinch or electrical stimulation of areas such as the pedunculopontine tegmental nucleus (Clement et al., 2008; Vanderwolf, 2003). This has led to the widespread use of urethane anesthesia as a model to study the effects of brain state on cortical processing (Castro-Alamancos, 2004b; Goard et al., 2009; Murakami et al., 2005). Even though the anesthetized cortex undoubtedly functions differently to the unanesthetized cortex, a variety of brain states can thus be found both within and without anesthesia. Conversely, cortical desynchronization is not necessary for behavioural consciousness, as evidenced by the presence of synchronized LFP patterns in actively behaving rats after blockade of neuromodulatory systems (Vanderwolf, 2000). While state-dependence of LFP patterns was established by classical studies (Vanderwolf, 2003), more recent work has shown that population spike patterns show similar state-dependence, with spontaneously population activity in the activated state showing no global fluctuations and extremely low of mean neuronal correlation. Remarkably, this can happen despite the strongly recurrent nature of cortical circuitry, which theoretical analyses suggest occurs because fluctuations arising from shared inputs are rapidly quashed by rapid inhibitory feedback (Renart et al., 2010).

A number of studies have shown that brain state can affect not just ongoing spontaneous activity but also sensory responses, in auditory as well as other cortices (Castro-Alamancos, 2004b; Edeline, 2003; Kisley et al., 1999; Worgotter et al., 1998). To investigate how brain state and spontaneous activity can influence auditory cortical population responses to acoustic stimuli, Curto et al (2009) recorded population activity together with local field potentials (LFPs), from layer 5 of auditory cortex of urethane-anesthetized rats. We recorded both spontaneous and click-evoked activity across a range of synchronized and desynchronized states, and focused our analysis on smoothed multi-unit activity (MUA) obtained by pooling together all spikes from simultaneously recorded neurons.

Global structure of population activity in auditory cortex

We began by visualizing how click responses vary with cortical state. First, we have to distinguish two slightly different uses of the word "state," corresponding to two different timescales. We shall refer to the state of the cortex, in the sense of the dynamics of network activity on a timescale of seconds or more and as reflected in the LFP power spectrum, as its *dynamic state;* the synchronized and desynchronized states are examples of dynamic states. The word "state" is also used to refer to fluctuations in instantaneous network activity at timescales of the order hundreds of milliseconds, as in the case of "upstates" and "downstates." We will use the term *activity state* to describe cortical states that persist on these shorter timescales.

To illustrate how sensory responses can depend on activity state at the time of stimulus presentation, Figure 9a shows population activity before and after six presentations of a click stimulus in a recording that was consistently in the synchronized state. In somatosensory cortex, whisker stimulation can "flip" neural activity from downstate to upstate and vice versa (Hasenstaub et al., 2007). Visual examination of our data suggested that click stimuli presented during the synchronized state can evoke a similar "flip" in auditory cortex. When the stimulus arrived during a downstate, an upstate frequently ensued (Figure 9a, trials 1-2). Similarly, stimuli that arrived during upstates could trigger downstates (Figure 9a, trials 5-6). Note that the initial response to the click (10-35ms; dark gray shading) was roughly similar across trials, whereas the persistent response (40-135ms; light gray shading) was more strongly modulated by the activity state at the time of the stimulus. We note that a number of previous studies have shown that cortical responses to sounds can be modulated by the history of previous stimuli, with stimulus-specific adaptation seen for stimuli presented up to tens of seconds previously (Ulanovsky et al., 2003; Ulanovsky et al., 2004). The effect we describe here however is different, being a modulation by only spontaneous activity, not dependent presentation of preceding stimuli.

To illustrate how dynamic state can affect click responses, Figure 9b shows data from a recording session whose dynamic state spontaneously varied from highly synchronized (trials 1-2) to highly desynchronized activity (trials 5-6). In these data, synchronized and desynchronized are not discrete cortical states, but rather extremes in a continuum. In the more synchronized cases (top), responses follow a pattern similar to that shown in Figure 9a. In desynchronized states however (bottom), the persistent response appears to be weakly modulated by the stimulus, instead returning to a baseline firing rate that matches the average firing rate preceding the stimulus (Curto et al., 2009).

A simple model of cortical state

Figure 9 suggests a complex dependence of sensory responses on dynamic and activity states at the time of stimulus presentation. However, this apparently complex relationship can be explained to a large extent by a simple principle, that sensory responses are shaped by the same dynamics that generate spontaneous activity prior to stimulus presentation. To show this, we predicted population sensory responses on individual trials, using a dynamical system model whose parameters were estimated from spontaneous activity preceding each stimulus.

In order to characterize the population dynamics, we first defined a variable $v(t)$ that measures the average population firing rate (represented by the red traces in Figure 9). To predict sensory activity, we used a dynamical system model, i.e. a differential equation giving the rate of change of $v(t)$ in terms of v, and another variable w which captures the degree to which recent spiking reduces network excitability. We found that the FitzHugh-Nagumo (FHN) equations (Fitzhugh, 1955) provided a simple family of self-exciting

dynamical systems yielding good approximations for the different dynamic states observed in our data, and also allowed simple and robust parameter estimation from small data segments. The FHN equations are:

$$\dot{v}=a_3v^3+a_2v^2+a_1v+bw+I+\varepsilon(t) \quad (1)$$

$$\dot{w}=(v-w)/\tau \quad (2)$$

The model parameters (a_1, a_2, a_3, b, and I), that specify how v and w evolve in time, correspond to its dynamic state. Note that while the FHN equations were originally used to model action potential generation in a single neuron, they are used here to model the mean activity of a population. For our purposes this is a phenomenological model; however it can also be interpreted mechanistically as a model of "mean field" network dynamics, where the mean rates of excitatory and inhibitory cells are both proportional to v, and w represents the combined effects of adaptive phenomena such as synaptic depression and cellular accommodation that reduce network excitability. In this scheme, the coefficients of the model can also be given mechanistic interpretations, with a_1, a_2, and a_3 corresponding to recurrent excitation and inhibition; b determining the extent to which increases in w reduce the excitability of the network; and I representing a constant 'tonic drive' on all cells, such as might arise from an increase in mean thalamic firing rates, or neuromodulatory activity that promotes tonic firing.

Model quantitatively predicts the structure of stimulus-evoked responses

To investigate whether the model could be used to quantitatively predict actual sensory responses on a trial-by-trial basis, we tested whether models fit on a short period (~3s) of spontaneous activity immediately preceding a stimulus were able to predict the structure of activity in the subsequent sensory response. The prediction methodology is illustrated in Figure 10a. A model fit from spontaneous activity preceding a stimulus yields an estimate of cortical state, including dynamic state (captured by model parameters a_1, a_2, a_3, b, I, illustrated by phase portrait) and activity state (v, w, illustrated by green star) at the time of the stimulus. A predicted response can be generated by solving the model equations with the fit parameters, using initial conditions given by the activity state, and driven by an alpha-function driving force $\varepsilon(t)$ without noise (Figure 10a, right).

Figure 10b shows model-based estimates of cortical state and predicted responses for each of the trials displayed in Figure 9a (left column). Visual inspection suggested that predicted responses (blue) typically closely matched actual responses (red) for a period of 100-200ms after click presentation. Later features of the response, such as "rebounds" from downstates that sometimes occurred ~200ms after click onset, were predicted with less accuracy. Because these trials all had similar dynamic state, there was relatively little variation in the model-fit phase portraits, and response variability was primarily explained by differences in activity state (green stars) at the time of the stimulus. Figure 10c shows the predictions of the model for the trials in Figure 9b, in which both dynamic and activity state were variable. Again, the model typically predicted the early component of the response well, with accuracy decaying after a period of 100-200ms. Model fits were not perfect: one feature that the model erroneously predicted was an induced suppression at ~100ms in the most desynchronized trials (Fig. 10c, bottom row). Nevertheless, despite its simplicity, the model appeared to capture the major features of cortical population responses across a range of dynamic states.

To quantify the ability of the models fit on each trial to predict the structure of the subsequent evoked response, we computed the driving force $\varepsilon(t)$ that would be necessary for the model to produce the actual response in the 300ms following the time of the stimulus. The integral of $\varepsilon^2(t)$ was used as a measure of how hard the model would have to be driven in order to exactly match the data; we call this the "prediction error." The smaller the prediction error, the more naturally the real response trajectory follows the model's prediction. By comparing the prediction error of the model fitted on spontaneous activity before a given trial, with the prediction errors of a null ensemble of models derived from other stimulus presentations, we were able to demonstrate the model's ability to capture the role of activity state and dynamic state in shaping click responses (Figs 10d-f; Curto et al., 2009). This suggests that sensory responses evolve according to the same cortical dynamics that govern the preceding spontaneous activity, and that these dynamics may be approximated by the FHN model family.

Further analyses (Curto et al 2009) suggested a possible interpretation for why this family of models was able to predict sensory responses. In synchronized states, dynamics were modeled by a self-exciting system, which can explain stimulus-induced "flipping" of up and downstates. According to the suggested interpretation of the model, self-excitation arises from recurrent excitation within cortex, counterbalanced by a build-up of adaptive processes such as synaptic depression and potassium channel activation, modeled by the *w* parameter. In downstates, *w* is small, and sensory stimulation triggers a rapid increase in *v* due to self-excitation. This leads to prolonged activity (an upstate), until *w* has increased enough to damp down the network's excitability. When stimuli are presented in an upstate, however, *v* is initially high and *w* of intermediate value, not yet enough to terminate the upstate. In this case, sensory stimulation causes a transient increase in *v*, followed by an increase in *w* which accelerates transition back to the downstate. During desynchronized states, model fits were closer to linear, with a single stable fixed point at intermediate values of *v* and *w*. In this state, stimuli caused reliable transient perturbations of both *v* and *w*, corresponding to the lower trial-to-trial variability seen in this state. A combination of recurrent excitation and network adaptation, with dynamics that vary with cortical state, may thus explain several features of cortical population dynamics.

In summary, the initial (~50ms) response of the population to click stimuli was largely independent of cortical state, while later response components showed a complex dependence on both dynamic and activity state, including "flip-flop" like behavior. Nevertheless, this apparently complex behavior could be explained by the simple principle that sensory responses evolve according to the same dynamics as spontaneous activity, using a low-dimensional dynamical system model to predict sensory responses on a trial-to-trial basis.

Conclusions and future questions

Although we now have a reasonable understanding of how individual neurons in auditory cortex represent simple sound stimuli, the task of understanding the way these individual neurons come together as a population is only just beginning. The simplest possibility would be that of *conditional independence*, in which case a complete description of population activity could be inferred from a knowledge of each neuron's relationship to sensory stimuli, with no coordination between neurons other than that induced by sensory stimuli themselves. This possibility corresponds basically to a framework proposed by Barlow (1972) under the name of the *Single Neuron Doctrine* (see Harris, 2005, for a more detailed discussion). Our data suggest that this picture is incomplete. The cortex can show structured activity patterns even in the absence of stimuli, and the pattern of background activity

present when a stimulus is presented appears to influence stimulus-induced activity, particularly for the extended (>~50ms) component of the response.

Similarities between evoked and spontaneous activity

When considering the initial response period, we observed many similarities between evoked responses and spontaneous activity. Within layer 5, we observed conserved constraints on the order in which neurons can fire, and also the combinations of neurons that can be simultaneously active. Looking across layers, we observed similarities in the sparseness profiles of different cell types, as well as variations between cells that at least morphologically appeared to belong to a single cell class.

What might cause these similarities? One can imagine a number of ways in which the properties of a neural circuit could impose constraints on the spike patterns it can generate. First, cortical neurons express diverse sets of voltage-gated ion channels, and are diverse in their intrinsic physiological properties even within a single cortical layer (Storm, 2000; Sugino et al., 2006), which may contribute to the diversity of timing profiles observed, and provide an explanation for why the timing profiles of individual cells should be similar across multiple stimuli. Second, connectivity within cortical circuits is far from homogenous; for example, strong reciprocal connectivity occurs more than expected by chance (Song et al., 2005). Such non-random connectivity patterns may impose constraints on the possible cell groups that can be active at any time. A number of differences have been found in the physiology and connectivity of different cortical cell classes, which may contribute to differing sparseness patterns between layers. For example, while lateral excitatory connections in deep layers are typically strong and widespread (Feldmeyer et al., 2006; Schubert et al., 2007; Thomson et al., 2007), the probability of PC-PC connections in L2/3 significantly decays over a spatial scale of 150 mm (Holmgren et al., 2003; Oswald et al., 2008) providing a potential mechanism for local clustering of superficial spiking activity at this scale. Furthermore, inhibitory inputs have been reported to be stronger onto L2/3 PCs than L5 PCs (van Brederode et al., 1995), with thick L5 PCs—for which we observed the densest activity—receiving weaker inhibition than slender PCs (Hefti et al., 2000; Hefti et al., 2003). Layer-specific features of excitatory and inhibitory circuits such as these may impose a consistent laminar structure on population activity patterns, whether evoked by auditory stimuli, or occurring spontaneously.

Beyond the initial period, responses were complex and highly variable between presentations of identical stimuli, at least in urethanized animals (Curto et al., 2009). However, much of this variability appears not to be random, but shows a systematic dependence on brain state and on the pattern of ongoing background activity when the stimulus was presented. We found that a simple self-exciting system model, whose dynamics was inferred from that of spontaneous activity immediately prior to the stimulus, could predict the late-period responses of layer 5 populations. This suggests that the complex form of the late-period responses may result from the same dynamical mechanisms that sculpt spontaneous activity.

Differences between evoked and spontaneous activity

The strong similarities between spontaneous and evoked activity are surprising, given that one would expect an animal should respond differently to a real sensory stimulus than to activity generated spontaneously within its own brain. So far we have identified two differences between evoked and spontaneous activity, both of which concern the manner in which activity propagates. Evoked activity appears first in thalamorecipient layers, and spreads quickly across columns; spontaneous activity appears first in deep layers and can spread more slowly across columns, sometimes appearing as a traveling wave (Luczak et al.,

2007). In principle, these differences could allow downstream neurons to distinguish true stimuli from spontaneous patterns. However, efferent projections from cortex can show laminar bias (subcortical projections, for example, arise from deep but not superficial layers), and a downstream neuron receiving inputs from only one layer could not distinguish relative laminar timing. It would be surprising, however, if the differences we have found so far turned out to be the only differences between spontaneous and evoked activity. For example, the methods we used to identify cells in vivo are crude; cortical cells can be highly diverse in terms of gene expression, even if morphologically similar (Arlotta et al., 2005; Sugino et al., 2006). Future technological developments that allow genetic identification of recorded neurons might reveal further differences between spontaneous and evoked activity.

The finding that evoked and spontaneous activity onsets propagate differently across cortical layers suggests that these types of activity are triggered by different mechanisms in vivo. Afferents from the ventral medial geniculate nucleus to primary auditory cortex terminate most densely in two laminar bands corresponding to lower L3/L4 and the L5/6 boundary (Kimura et al., 2003; Romanski et al., 1993). We found that the earliest sensory-evoked responses are found in the middle layers and a restricted portion of the lower layers, which correspond on an experiment-to-experiment basis with the locations of early sinks measured by current source density analysis (Kaur et al., 2005; Sakata et al., 2009, supplementary Figures S10 and S16). Our data are therefore consistent with an initiation of sensory-evoked activity in the thalamorecipient layers. We note that PCs can receive excitatory inputs all along their dendritic length and that thalamic inputs could in principle provide excitation to neurons of other laminae (Bureau et al., 2006). Earlier sensory responses in cells of thalamorecipient layers might however reflect these cells receiving stronger excitatory drive, perhaps due to excitation proximal to the soma. While we observed spontaneous activity to often spread as a traveling wave, sensory responses appeared almost simultaneously across the cortical surface. This pattern of sensory responses is therefore consistent with divergent and broadly tuned thalamocortical input, a result also suggested by the persistence of broadly tuned responses after inhibition of spiking in auditory cortex (Liu et al., 2007). The observed spread of upstates is consistent with in vitro models, which show generation and spread of spontaneous activity in deep layers (Sanchez-Vives et al., 2000). Deep layers are a major target of “feedback” projections from higher cortical areas (Felleman et al., 1991; Rouiller et al., 1991). The fact that auditory cortical upstates were first seen in deep layers is thus consistent with a role of projections from higher cortical regions in initiating spontaneous patterns in primary sensory cortex, consistent with their proposed role in processes such as memory replay (Buzsaki, 1989; Hoffman et al., 2007; Marr, 1971).

Implications for cortical processing in behaving animals

The above data was collected in either urethane-anesthetized or unanesthetized passively listening animals. Brain state changes occur spontaneously in both these conditions, and research in somatosensory cortex suggests that the variations in brain state seen under urethane can form a good model for variations in brain state found between behavioral conditions (Castro-Alamancos, 2004a). Clearly, however, an important topic for future research is to study population-level activity in auditory cortex of actively behaving animals. At present we can only speculate what the results of such studies might be. We would like to suggest two possibilities.

The first possibility is that the structure of cortical activity might actually be simpler in actively behaving than in passively listening animals. We found that in the most activated states under urethane, background activity was largely unstructured and sensory responses were more reliable and repeatable between stimulus presentations. Perhaps in an animal that is highly attentive to acoustic stimuli, auditory cortex will exhibit a constant activated state,

thereby forming a faithful representation of external stimuli in which responses are conditionally independent, i.e. in which the single neuron doctrine holds (Barlow, 1972; Harris, 2005).

The second possibility, however, is that variability and state-dependence of sensory responses is actually fundamental to cortical information processing. In this view, the role of sensory cortex is not just to represent external stimuli, but to actively transform them in a way that depends on context, e.g. the cognitive state of the animal. A number of studies have shown that spiking activity in auditory and other sensory cortices can be modulated by multimodal, nonsensory, and cognitive variables (Brosch et al., 2005; Lakatos et al., 2007; Shuler et al., 2006), presumably reflecting the influence of “top-down” inputs from higher cortical structures. In anesthetized subjects we found that spontaneous activity prior to stimulus presentation modulated sensory responses, and that this modulation was strongest for the late period responses (>50ms after stimulus onset). If similar processes occur in behaving animals, it would suggest that top-down inputs, by establishing an appropriate pattern of ongoing activity, could shape the response to subsequent sensory stimuli. We note that a number of studies in behaving animals have shown that while early period responses tend to faithfully reflect sensory inputs, late-period responses also reflect other features such as attention, categories and behavioural choices (Brincat et al., 2006; Cohen et al., 2009; Jeschke et al., 2008; John et al., 1973; Ohl et al., 2001; Scheich et al., 2007; Sugase et al., 1999). The behaviour produced by an animal is likewise shaped not only by immediate sensory stimuli, but also by the cognitive context in which they occur. The dependence of late period responses on prior activity might thus be a signature of a computation in which stimuli and context come together to produce appropriate behaviour.

References

Arlotta P, Molyneaux BJ, Chen J, Inoue J, Kominami R, Macklis JD. Neuronal subtype-specific genes that control corticospinal motor neuron development in vivo. Neuron 2005;45:207–221. [PubMed: 15664173]

Atencio CA, Schreiner CE. Laminar diversity of dynamic sound processing in cat primary auditory cortex. J Neurophysiol 2010;103:192–205. [PubMed: 19864440]

Bandyopadhyay S, Shamma SA, Kanold PO. Dichotomy of functional organization in the mouse auditory cortex. Nat Neurosci 2010;13:361–368. [PubMed: 20118924]

Barbour DL, Callaway EM. Excitatory local connections of superficial neurons in rat auditory cortex. J Neurosci 2008;28:11174–85. [PubMed: 18971460]

Barlow HB. Single units and sensation: a neuron doctrine for perceptual psychology? Perception 1972;1:371–394. [PubMed: 4377168]

Bartho P, Curto C, Luczak A, Marguet SL, Harris KD. Population coding of tone stimuli in auditory cortex: dynamic rate vector analysis. Eur J Neurosci 2009;30:1767–78. [PubMed: 19840110]

Bartho P, Hirase H, Monconduit L, Zugaro M, Harris KD, Buzsaki G. Characterization of neocortical principal cells and interneurons by network interactions and extracellular features. J Neurophysiol 2004;92:600–608. [PubMed: 15056678]

Berke JD, Okatan M, Skurski J, Eichenbaum HB. Oscillatory entrainment of striatal neurons in freely moving rats. Neuron 2004;43:883–96. [PubMed: 15363398]

Brincat SL, Connor CE. Dynamic shape synthesis in posterior inferotemporal cortex. Neuron 2006;49:17–24. [PubMed: 16387636]

Brosch M, Schreiner CE. Correlations between neural discharges are related to receptive field properties in cat primary auditory cortex. Eur J Neurosci 1999;11:3517–30. [PubMed: 10564360]

Brosch M, Selezneva E, Scheich H. Nonauditory events of a behavioral procedure activate auditory cortex of highly trained monkeys. J Neurosci 2005;25:6797–6806. [PubMed: 16033889]

Bureau I, von Saint Paul F, Svoboda K. Interdigitated paralemniscal and lemniscal pathways in the mouse barrel cortex. PLoS Biol 2006;4:e382. [PubMed: 17121453]

Buzsaki G. Two-stage model of memory trace formation: a role for 'noisy' brain states. Neuroscience 1989;31:551–70. [PubMed: 2687720]

Buzsaki G, Bickford RG, Ponomareff G, Thal LJ, Mandel R, Gage FH. Nucleus basalis and thalamic control of neocortical activity in the freely moving rat. J Neurosci 1988;8:4007–26. [PubMed: 3183710]

Castro-Alamancos MA. Absence of rapid sensory adaptation in neocortex during information processing states. Neuron 2004a;41:455–64. [PubMed: 14766183]

Castro-Alamancos MA. Dynamics of sensory thalamocortical synaptic networks during information processing states. Prog Neurobiol 2004b;74:213–247. [PubMed: 15556288]

Chauvette S, Volgushev M, Timofeev I. Origin of Active States in Local Neocortical Networks during Slow Sleep Oscillation. Cereb Cortex. 2010

Clement EA, Richard A, Thwaites M, Ailon J, Peters S, Dickson CT. Cyclic and sleep-like spontaneous alternations of brain state under urethane anaesthesia. PLoS ONE 2008;3:e2004. [PubMed: 18414674]

Cohen MR, Maunsell JH. Attention improves performance primarily by reducing interneuronal correlations. Nat Neurosci 2009;12:1594–1600. [PubMed: 19915566]

Csicsvari J, Henze DA, Jamieson B, Harris KD, Sirota A, Bartho P, Wise KD, Buzsaki G. Massively parallel recording of unit and local field potentials with silicon-based electrodes. Journal of Neurophysiology 2003;90:1314–1323. [PubMed: 12904510]

Curto C, Sakata S, Marguet S, Itskov V, Harris KD. A simple model of cortical dynamics explains variability and state dependence of sensory responses in urethane-anesthetized auditory cortex. J Neurosci 2009;29:10600–12. [PubMed: 19710313]

deCharms RC, Merzenich MM. Primary cortical representation of sounds by the coordination of action- potential timing. Nature 1996;381:610–613. [PubMed: 8637597]

DeWeese MR, Wehr M, Zador AM. Binary spiking in auditory cortex. J Neurosci 2003;23:7940–7949. [PubMed: 12944525]

Edeline JM. The thalamo-cortical auditory receptive fields: regulation by the states of vigilance, learning and the neuromodulatory systems. Exp Brain Res 2003;153:554–72. [PubMed: 14517594]

Eggermont JJ. Properties of correlated neural activity clusters in cat auditory cortex resemble those of neural assemblies. J Neurophysiol 2006;96:746–64. [PubMed: 16835364]

Einevoll GT, Pettersen KH, Devor A, Ulbert I, Halgren E, Dale AM. Laminar population analysis: estimating firing rates and evoked synaptic activity from multielectrode recordings in rat barrel cortex. J Neurophysiol 2007;97:2174–2190. [PubMed: 17182911]

Feldmeyer D, Lubke J, Sakmann B. Efficacy and connectivity of intracolumnar pairs of layer 2/3 pyramidal cells in the barrel cortex of juvenile rats. J Physiol 2006;575:583–602. [PubMed: 16793907]

Felleman DJ, Van Essen DC. Distributed hierarchical processing in the primate cerebral cortex. Cereb Cortex 1991;1:1–47. [PubMed: 1822724]

Felsen G, Mainen ZF. Neural substrates of sensory-guided locomotor decisions in the rat superior colliculus. Neuron 2008;60:137–48. [PubMed: 18940594]

Fries P, Reynolds JH, Rorie AE, Desimone R. Modulation of oscillatory neuronal synchronization by selective visual attention. Science 2001;291:1560–1563. [PubMed: 11222864]

Gerstein GL, Perkel DH, Dayhoff JE. Cooperative firing activity in simultaneously recorded populations of neurons: detection and measurement. J Neurosci 1985;5:881–9. [PubMed: 3981248]

Goard M, Dan Y. Basal forebrain activation enhances cortical coding of natural scenes. Nat Neurosci 2009;12:1444–9. [PubMed: 19801988]

Gray CM, Maldonado PE, Wilson M, McNaughton B. Tetrodes markedly improve the reliability and yield of multiple single-unit isolation from multi-unit recordings in cat striate cortex. J Neurosci Methods 1995;63:43–54. [PubMed: 8788047]

Haider B, Duque A, Hasenstaub AR, Yu Y, McCormick DA. Enhancement of visual responsiveness by spontaneous local network activity in vivo. J Neurophysiol 2007;97:4186–4202. [PubMed: 17409168]

Harris KD. Neural signatures of cell assembly organization. Nat Rev Neurosci 2005;6:399–407. [PubMed: 15861182]

Harris KD, Henze DA, Csicsvari J, Hirase H, Buzsaki G. Accuracy of tetrode spike separation as determined by simultaneous intracellular and extracellular measurements. J Neurophysiol 2000;84:401–414. [PubMed: 10899214]

Hasenstaub A, Sachdev RN, McCormick DA. State changes rapidly modulate cortical neuronal responsiveness. J Neurosci 2007;27:9607–9622. [PubMed: 17804621]

Hefti BJ, Smith PH. Anatomy, physiology, and synaptic responses of rat layer V auditory cortical cells and effects of intracellular GABA(A) blockade. J Neurophysiol 2000;83:2626–2638. [PubMed: 10805663]

Hefti BJ, Smith PH. Distribution and kinetic properties of GABAergic inputs to layer V pyramidal cells in rat auditory cortex. J Assoc Res Otolaryngol 2003;4:106–121. [PubMed: 12209293]

Heil P. First-spike latency of auditory neurons revisited. Curr Opin Neurobiol 2004;14:461–467. [PubMed: 15321067]

Hoffman KL, McNaughton BL. Coordinated reactivation of distributed memory traces in primate neocortex. Science 2002;297:2070–2073. [PubMed: 12242447]

Hoffman KL, Battaglia FP, Harris K, MacLean JN, Marshall L, Mehta MR. The upshot of up states in the neocortex: from slow oscillations to memory formation. J Neurosci 2007;27:11838–11841. [PubMed: 17978020]

Holmgren C, Harkany T, Svennenfors B, Zilberter Y. Pyramidal cell communication within local networks in layer 2/3 of rat neocortex. J Physiol 2003;551:139–53. [PubMed: 12813147]

Hromadka T, Deweese MR, Zador AM. Sparse representation of sounds in the unanesthetized auditory cortex. PLoS Biol 2008;6:e16. [PubMed: 18232737]

Jermakowicz WJ, Chen X, Khaytin I, Bonds AB, Casagrande VA. Relationship between spontaneous and evoked spike-time correlations in primate visual cortex. J Neurophysiol 2009;101:2279–89. [PubMed: 19211656]

Jeschke M, Lenz D, Budinger E, Herrmann CS, Ohl FW. Gamma oscillations in gerbil auditory cortex during a target-discrimination task reflect matches with short-term memory. Brain Res 2008;1220:70–80. [PubMed: 18053969]

John ER, Bartlett F, Shimokochi M, Kleinman D. Neural readout from memory. J Neurophysiol 1973;36:893–924. [PubMed: 4805018]

Kandel A, Buzsaki G. Cellular-synaptic generation of sleep spindles, spike-and-wave discharges, and evoked thalamocortical responses in the neocortex of the rat. J Neurosci 1997;17:6783–97. [PubMed: 9254689]

Katzner S, Nauhaus I, Benucci A, Bonin V, Ringach DL, Carandini M. Local origin of field potentials in visual cortex. Neuron 2009;61:35–41. [PubMed: 19146811]

Kaur S, Rose HJ, Lazar R, Liang K, Metherate R. Spectral integration in primary auditory cortex: laminar processing of afferent input, in vivo and in vitro. Neuroscience 2005;134:1033–1045. [PubMed: 15979241]

Kimura A, Donishi T, Sakoda T, Hazama M, Tamai Y. Auditory thalamic nuclei projections to the temporal cortex in the rat. Neuroscience 2003;117:1003–16. [PubMed: 12654352]

Kisley MA, Gerstein GL. Trial-to-trial variability and state-dependent modulation of auditory-evoked responses in cortex. J Neurosci 1999;19:10451–60. [PubMed: 10575042]

Kosslyn SM, Ganis G, Thompson WL. Neural foundations of imagery. Nat Rev Neurosci 2001;2:635–642. [PubMed: 11533731]

Kraemer DJ, Macrae CN, Green AE, Kelley WM. Musical imagery: sound of silence activates auditory cortex. Nature 2005;434:158. [PubMed: 15758989]

Kreiman G, Koch C, Fried I. Imagery neurons in the human brain. Nature 2000;408:357–361. [PubMed: 11099042]

Kruskal, JB.; Wish, M. Multidimensional scaling. Sage Publications; Beverly Hills, Calif.: 1978.

Lakatos P, Chen CM, O'Connell MN, Mills A, Schroeder CE. Neuronal oscillations and multisensory interaction in primary auditory cortex. Neuron 2007;53:279–92. [PubMed: 17224408]

Laurent G. Olfactory network dynamics and the coding of multidimensional signals. Nat Rev Neurosci 2002;3:884–895. [PubMed: 12415296]

Linden JF, Schreiner CE. Columnar transformations in auditory cortex? A comparison to visual and somatosensory cortices Cereb Cortex 2003;13:83–89.

Liu BH, Wu GK, Arbuckle R, Tao HW, Zhang LI. Defining cortical frequency tuning with recurrent excitatory circuitry. Nat Neurosci 2007;10:1594–600. [PubMed: 17994013]

Logothetis NK, Pauls J, Augath M, Trinath T, Oeltermann A. Neurophysiological investigation of the basis of the fMRI signal. Nature 2001;412:150–7. [PubMed: 11449264]

Luczak A, Bartho P, Harris KD. Spontaneous events outline the realm of possible sensory responses in neocortical populations. Neuron 2009;62:413–25. [PubMed: 19447096]

Luczak A, Bartho P, Marguet SL, Buzsaki G, Harris KD. Sequential structure of neocortical spontaneous activity in vivo. Proc Natl Acad Sci USA 2007;104:347–352. [PubMed: 17185420]

Marr D. Simple memory: a theory for archicortex. Philos Trans R Soc Lond B Biol Sci 1971;262:23–81. [PubMed: 4399412]

McNaughton BL, O'Keefe J, Barnes CA. The stereotrode: a new technique for simultaneous isolation of several single units in the central nervous system from multiple unit records. J Neurosci Methods 1983;8:391–397. [PubMed: 6621101]

Mitchell JF, Sundberg KA, Reynolds JH. Spatial attention decorrelates intrinsic activity fluctuations in macaque area V4. Neuron 2009;63:879–88. [PubMed: 19778515]

Mitzdorf U. Current source-density method and application in cat cerebral cortex: investigation of evoked potentials and EEG phenomena. Physiol Rev 1985;65:37–100. [PubMed: 3880898]

Moshitch D, Las L, Ulanovsky N, Bar-Yosef O, Nelken I. Responses of neurons in primary auditory cortex (A1) to pure tones in the halothane-anesthetized cat. J Neurophysiol 2006;95:3756–3769. [PubMed: 16554513]

Murakami M, Kashiwadani H, Kirino Y, Mori K. State-dependent sensory gating in olfactory cortex. Neuron 2005;46:285–96. [PubMed: 15848806]

Ohl FW, Scheich H, Freeman WJ. Change in pattern of ongoing cortical activity with auditory category learning. Nature 2001;412:733–6. [PubMed: 11507640]

Oram MW, Xiao D, Dritschel B, Payne KR. The temporal resolution of neural codes: does response latency have a unique role? Philos Trans R Soc Lond B Biol Sci 2002;357:987–1001. [PubMed: 12217170]

Oswald AM, Reyes AD. Maturation of intrinsic and synaptic properties of layer 2/3 pyramidal neurons in mouse auditory cortex. J Neurophysiol 2008;99:2998–3008. [PubMed: 18417631]

Oswald AM, Doiron B, Rinzel J, Reyes AD. Spatial profile and differential recruitment of GABAB modulate oscillatory activity in auditory cortex. J Neurosci 2009;29:10321–34. [PubMed: 19692606]

Pesaran B, Pezaris JS, Sahani M, Mitra PP, Andersen RA. Temporal structure in neuronal activity during working memory in macaque parietal cortex. Nat Neurosci 2002;5:805–11. [PubMed: 12134152]

Petersen CC, Hahn TT, Mehta M, Grinvald A, Sakmann B. Interaction of sensory responses with spontaneous depolarization in layer 2/3 barrel cortex. Proc Natl Acad Sci USA 2003;100:13638–13643. [PubMed: 14595013]

Pinault D. A novel single-cell staining procedure performed in vivo under electrophysiological control: morpho-functional features of juxtacellularly labeled thalamic cells and other central neurons with biocytin or Neurobiotin. J Neurosci Methods 1996;65:113–36. [PubMed: 8740589]

Poulet JF, Petersen CC. Internal brain state regulates membrane potential synchrony in barrel cortex of behaving mice. Nature 2008;454:881–5. [PubMed: 18633351]

Ranade SP, Mainen ZF. Transient firing of dorsal raphe neurons encodes diverse and specific sensory, motor, and reward events. J Neurophysiol 2009;102:3026–37. [PubMed: 19710375]

Recce M, O'Keefe J. The tetrode: a new technique for multi-unit extracellular recording. Soc Neurosci Abstr 1989;15:1250.

Renart A, de la Rocha J, Bartho P, Hollender L, Parga N, Reyes A, Harris KD. The asynchronous state in cortical circuits. Science 2010;327:587–90. [PubMed: 20110507]

Romanski LM, LeDoux JE. Organization of rodent auditory cortex: anterograde transport of PHA-L from MGv to temporal neocortex. Cereb Cortex 1993;3:499–514. [PubMed: 7511011]

Rothschild G, Nelken I, Mizrahi A. Functional organization and population dynamics in the mouse primary auditory cortex. Nat Neurosci 2010;13:353–60. [PubMed: 20118927]

Rouiller EM, Simm GM, Villa AE, de Ribaupierre Y, de Ribaupierre F. Auditory corticocortical interconnections in the cat: evidence for parallel and hierarchical arrangement of the auditory cortical areas. Exp Brain Res 1991;86:483–505. [PubMed: 1722171]

Sakata S, Harris KD. Laminar structure of spontaneous and sensory-evoked population activity in auditory cortex. Neuron 2009;64:404–18. [PubMed: 19914188]

Sally SL, Kelly JB. Organization of auditory cortex in the albino rat: sound frequency. J Neurophysiol 1988;59:1627–1638. [PubMed: 3385476]

Sanchez-Vives MV, McCormick DA. Cellular and network mechanisms of rhythmic recurrent activity in neocortex. Nat Neurosci 2000;3:1027–1034. [PubMed: 11017176]

Scheich H, Brechmann A, Brosch M, Budinger E, Ohl FW. The cognitive auditory cortex: task-specificity of stimulus representations. Hear Res 2007;229:213–224. [PubMed: 17368987]

Schmitzer-Torbert N, Jackson J, Henze D, Harris K, Redish AD. Quantitative measures of cluster quality for use in extracellular recordings. Neuroscience 2005;131:1–11. [PubMed: 15680687]

Schubert D, Kotter R, Staiger JF. Mapping functional connectivity in barrel-related columns reveals layer- and cell type-specific microcircuits. Brain Struct Funct 2007;212:107–19. [PubMed: 17717691]

Shuler MG, Bear MF. Reward timing in the primary visual cortex. Science 2006;311:1606–1609. [PubMed: 16543459]

Smith PH, Populin LC. Fundamental differences between the thalamocortical recipient layers of the cat auditory and visual cortices. J Comp Neurol 2001;436:508–519. [PubMed: 11447593]

Song S, Sjostrom PJ, Reigl M, Nelson S, Chklovskii DB. Highly nonrandom features of synaptic connectivity in local cortical circuits. PLoS Biol 2005;3:e68. [PubMed: 15737062]

Steriade M, McCormick DA, Sejnowski TJ. Thalamocortical oscillations in the sleeping and aroused brain. Science 1993a;262:679–85. [PubMed: 8235588]

Steriade M, Nunez A, Amzica F. A novel slow (< 1 Hz) oscillation of neocortical neurons in vivo: depolarizing and hyperpolarizing components. J Neurosci 1993b;13:3252–65. [PubMed: 8340806]

Steriade M, Timofeev I, Grenier F. Natural waking and sleep states: a view from inside neocortical neurons. J Neurophysiol 2001;85:1969–1985. [PubMed: 11353014]

Stopfer M, Jayaraman V, Laurent G. Intensity versus identity coding in an olfactory system. Neuron 2003;39:991–1004. [PubMed: 12971898]

Storm JF. K(+) channels and their distribution in large cortical pyramidal neurones. J Physiol 2000;525(Pt 3):565–6. [PubMed: 10856111]

Sugase Y, Yamane S, Ueno S, Kawano K. Global and fine information coded by single neurons in the temporal visual cortex. Nature 1999;400:869–873. [PubMed: 10476965]

Sugino K, Hempel CM, Miller MN, Hattox AM, Shapiro P, Wu C, Huang ZJ, Nelson SB. Molecular taxonomy of major neuronal classes in the adult mouse forebrain. Nat Neurosci 2006;9:99–107. [PubMed: 16369481]

Szymanski FD, Garcia-Lazaro JA, Schnupp JW. Current source density profiles of stimulus-specific adaptation in rat auditory cortex. J Neurophysiol 2009;102:1483–90. [PubMed: 19571199]

Thomson AM, Lamy C. Functional maps of neocortical local circuitry. Front Neurosci 2007;1:19–42. [PubMed: 18982117]

Ulanovsky N, Las L, Nelken I. Processing of low-probability sounds by cortical neurons. Nat Neurosci 2003;6:391–8. [PubMed: 12652303]

Ulanovsky N, Las L, Farkas D, Nelken I. Multiple time scales of adaptation in auditory cortex neurons. J Neurosci 2004;24:10440–53. [PubMed: 15548659]

van Brederode JF, Spain WJ. Differences in inhibitory synaptic input between layer II-III and layer V neurons of the cat neocortex. J Neurophysiol 1995;74:1149–1166. [PubMed: 7500140]

Vanderwolf CH. Are neocortical gamma waves related to consciousness? Brain Res 2000;855:217–24. [PubMed: 10677593]

Vanderwolf, CH. An odyssey through the brain, behavior, and the mind. Kluwer Academic Pub; Boston: 2003.

Volkov IO, Galazjuk AV. Formation of spike response to sound tones in cat auditory cortex neurons: interaction of excitatory and inhibitory effects. Neuroscience 1991;43:307–21. [PubMed: 1922775]

Wallace MN, Palmer AR. Laminar differences in the response properties of cells in the primary auditory cortex. Exp Brain Res 2008;184:179–91. [PubMed: 17828392]

Wang X, Lu T, Snider RK, Liang L. Sustained firing in auditory cortex evoked by preferred stimuli. Nature 2005;435:341–346. [PubMed: 15902257]

Wiest MC, Nicolelis MA. Behavioral detection of tactile stimuli during 7-12 Hz cortical oscillations in awake rats. Nat Neurosci 2003;6:913–914. [PubMed: 12897789]

Winer JA, Lee CC. The distributed auditory cortex. Hear Res 2007;229:3–13. [PubMed: 17329049]

Worgotter F, Suder K, Zhao Y, Kerscher N, Eysel UT, Funke K. State-dependent receptive-field restructuring in the visual cortex. Nature 1998;396:165–8. [PubMed: 9823895]

Zhou Y, Liu BH, Wu GK, Kim YJ, Xiao Z, Tao HW, Zhang LI. Preceding inhibition silences layer 6 neurons in auditory cortex. Neuron 2010;65:706–17. [PubMed: 20223205]

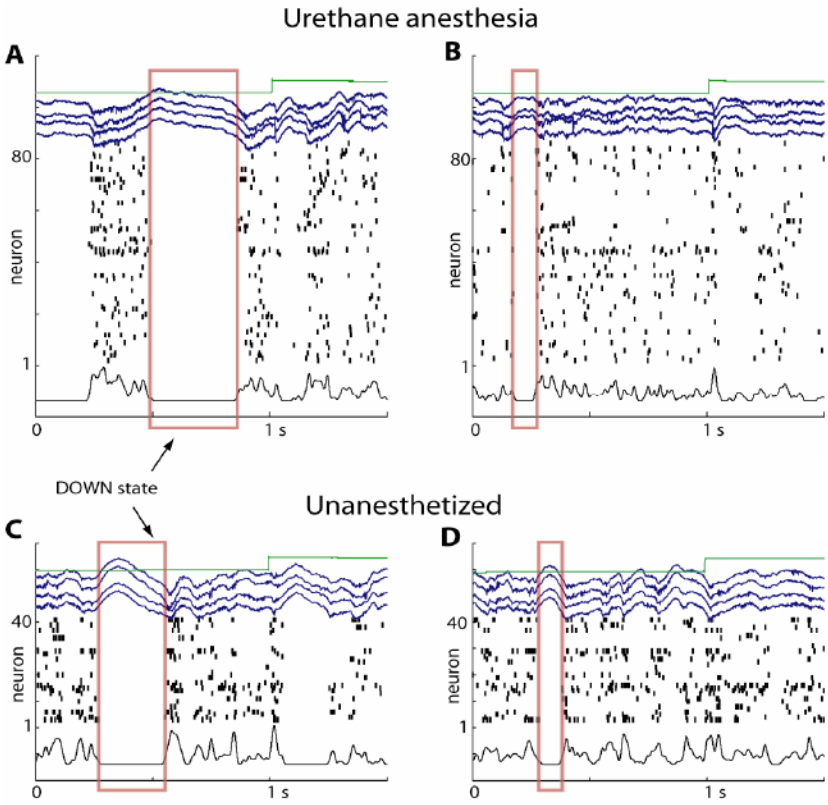

Figure 1. Structured spontaneous activity in auditory cortex

Raster plots show activity of simultaneously recorded layer 5 neurons, blue traces show local field potentials (LFP) recorded from the a subset of the channels from which spikes were detected. Bottom black trace indicates multiunit activity (MUA), i.e. the population-averaged firing rate of all recorded cells. Red rectangles indicate "downstates," i.e. periods of global network silence. Green traces show sync pulses, with positive values indicating times of tone presentation. **(A, B)** show two periods from a single recording under urethane anesthesia, **(C, D)** show two periods in a passively listening unanesthetized animal. Note that structured population activity is seen in all cases, but that the nature of this activity (such as the length of downstates) is variable both between and within recordings. Adapted from Luczak et al (2009).

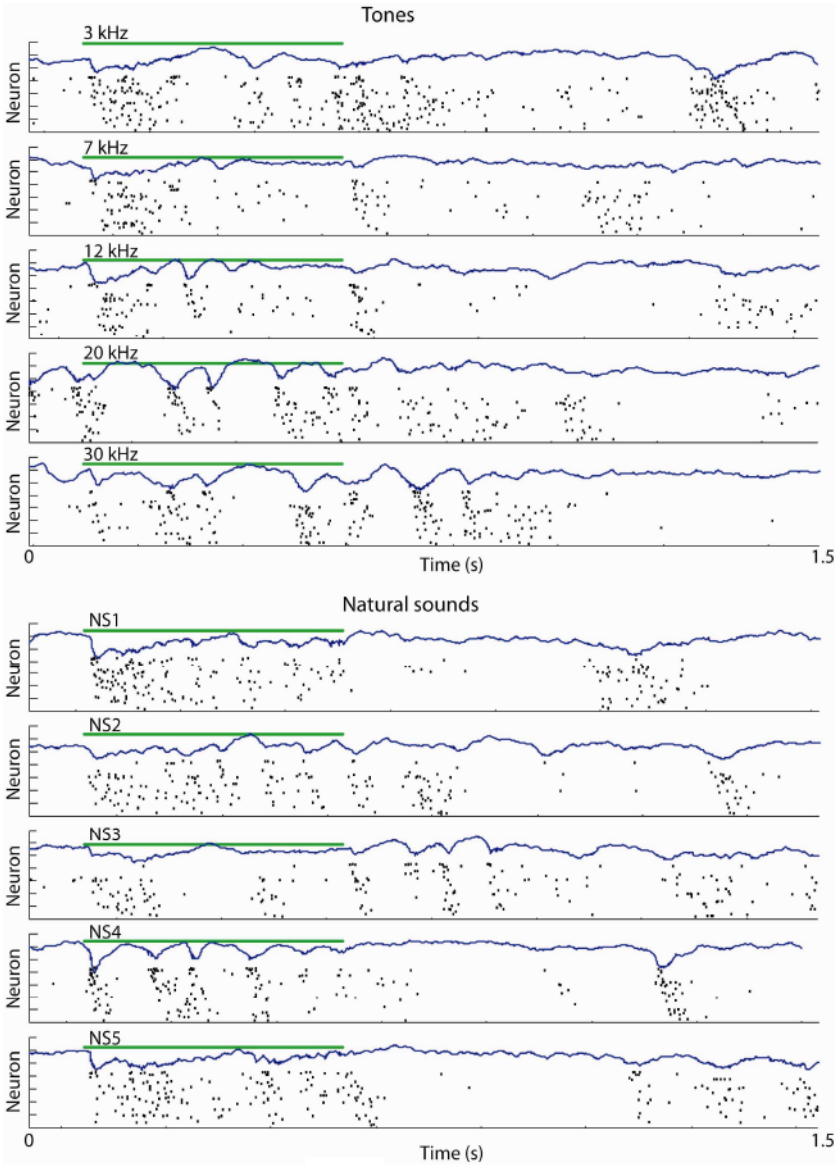

Figure 2. Sequential population activity patterns

Representative raw data plots, showing responses to five tones (3, 7, 12, 20, 30 kHz respectively) and five different natural sounds (insect vocalizations), together with spontaneous activity patterns seen after stimulus offset, taken from a single recording under urethane. The green line indicates the duration of the stimulus; blue traces show local field potentials from one of the recording sites; underneath is a raster plot showing the spike trains of simultaneously recorded neurons. Neurons are sorted vertically by average spontaneous mean spike latency to reveal sequential firing patterns (unlike Figure 1, where they were arranged by recording shank). Neurons are displayed in the same vertical order in all plots. Although population firing events can vary significantly in firing rate and duration, stereotyped sequential patterns of timescale ~100ms typically accompany evoked and spontaneous population spiking events, as well as occurring during the presentation of extended tones and natural sounds. Adapted from Luczak et al (2009).

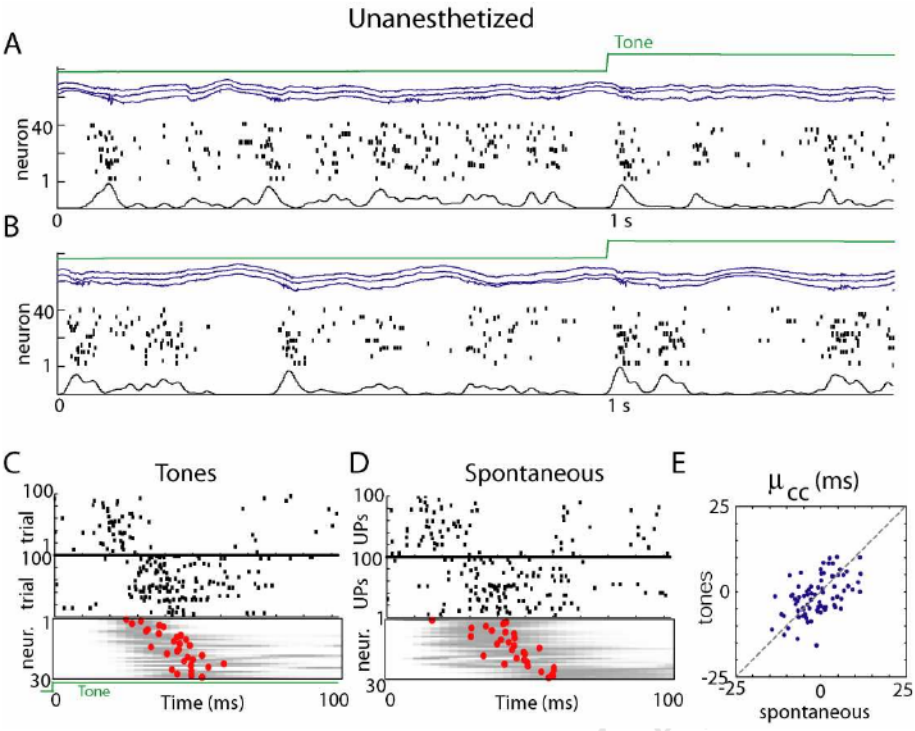

Figure 3. Preservation of sequential structure between sensory-evoked and spontaneous events in unanesthetized animals

(**A, B**) Representative raw data plots from an unanesthetized, head-fixed subject in a passive listening paradigm. (**C,D**) Top two rasters (black ticks) show spike times for two individual neurons, triggered by tone onsets (C) and upstate onsets (D). Bottom panels show average activity of all simultaneously recorded neurons triggered by tone or upstate onsets: grey bars show pseudocolor representations of each neuron's perievent time histogram (PETH), red dots denote each neuron's mean spike latency in the 100ms after tone onset. Neurons are ordered vertically by the mean latency over all stimuli, to illustrate sequential spread of activity. Neurons are sorted in the same order in C and D, to illustrate the similar sequential order of tone-evoked and spontaneous activity. (**E**) Conservation of latency measure μ_{cc} across tones and spontaneous events. Adapted from Luczak et al (2009).

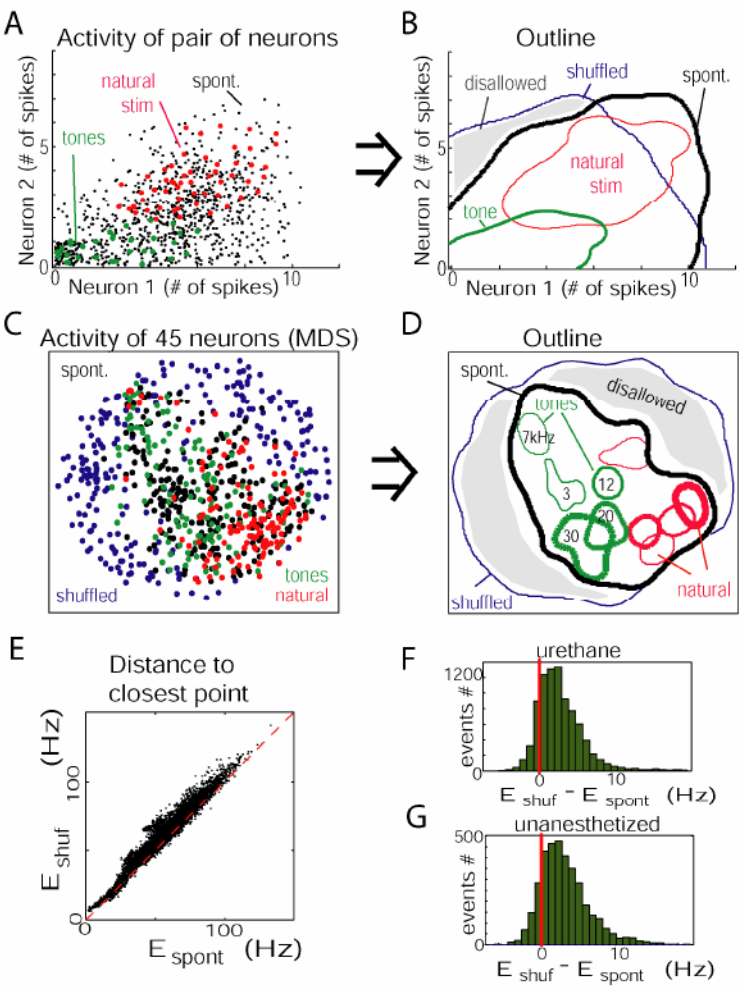

Figure 4. Combinatorial constraints on population firing rate vectors

(**A**) Spike counts of two neurons (recorded from separate tetrodes) during the first 100ms of spontaneous upstates (black), responses to a tone (green), and natural sound (red). Data were jittered to show overlapping points. Note that regions occupied by responses to the sensory stimuli differ, but are both contained in the realm outlined by spontaneous patterns. (**B**) Contour plot showing regions occupied by points from (A). The blue outline is computed from spike counts shuffled between upstates, indicating the region that would be occupied in the absence of spike count correlations. (**C**) Firing rate vectors of entire population, visualized using multidimensional scaling; each dot represents the activity of 45 neurons, nonlinearly projected into two-dimensional space. (**D**) Contour plot derived from multidimensional scaling data, with responses to individual stimuli marked separately. Sensory-evoked responses again lie within the realm outlined by spontaneous events. (**E**) Scatter plot showing the Euclidean distances from each evoked event to its closest neighbor in the spontaneous events (E_{spont}), and in the shuffled spontaneous events (E_{shuf}). Dashed red line shows equality. (**F, G**) Histogram showing the difference between distances to shuffled and spontaneous events (E_{shuf} - E_{spont}). Top and bottom: data from all anesthetized and unanesthetized experiments, respectively. Almost every evoked event was closer to a true spontaneous vector than to a shuffled vector. Adapted from Luczak et al (2009).

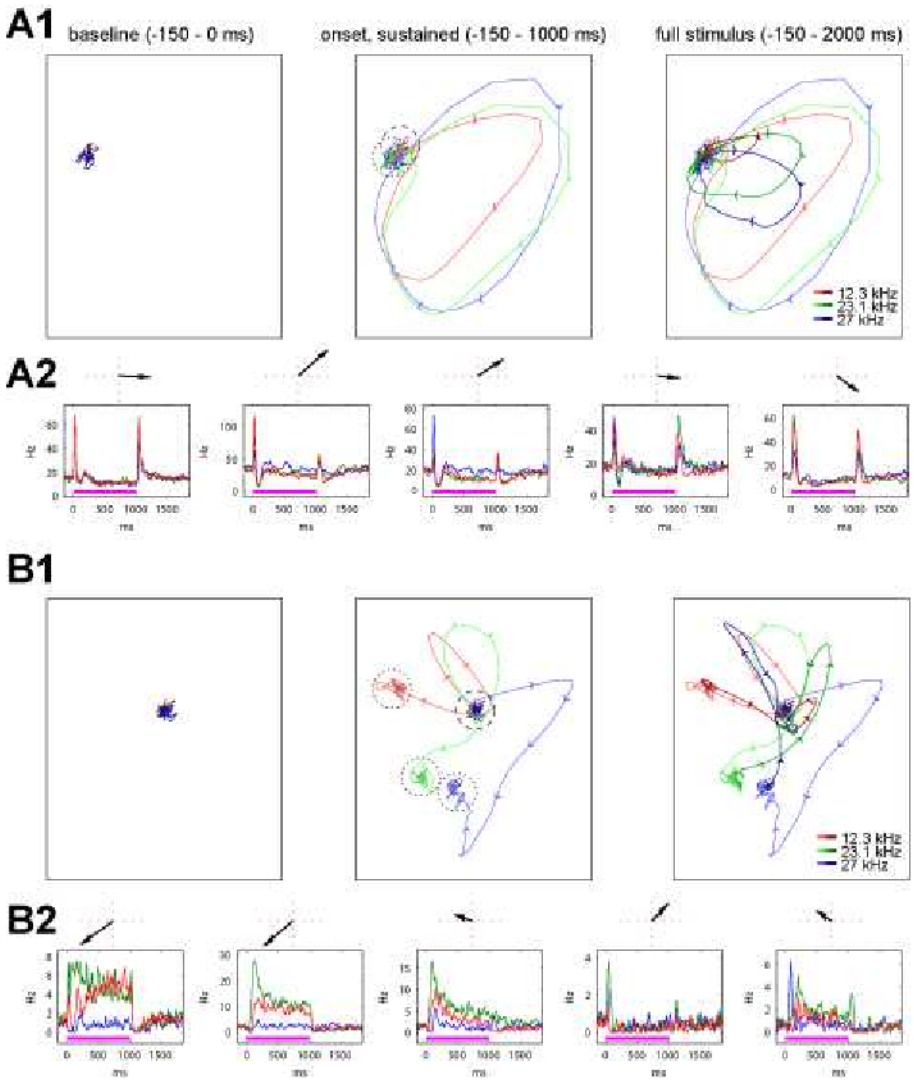

Figure 5. Visualization of population firing rate vectors

The panels show projections of the mean firing rate vector trajectory of 282 cells pooled from 4 experiments, evoked by tones of three frequencies, plotted for increasingly longer time periods from left to right. (**A1**) Trajectories viewed with principal component analysis (PCA), which finds the projection of maximum variance; all three plots are in the same projection. In this projection, onset responses are dominant. (**A2**) PSTHs of the five cells contributing most to the PCA projection. Arrows above each PSTH indicate factor loadings in the projections above. (**B1**) Trajectories viewed with multiple discriminant analysis (MDA), to maximize the differences between sustained responses. In this projection, onset, sustained, and offset responses have approximately equal magnitude. Dashed circles: baseline activity, dotted circles: sustained activity. (**B2**) PSTHs of the five cells contributing most to the MDA projection. Arrows as in A2. Adapted from Bartho et al (2009).

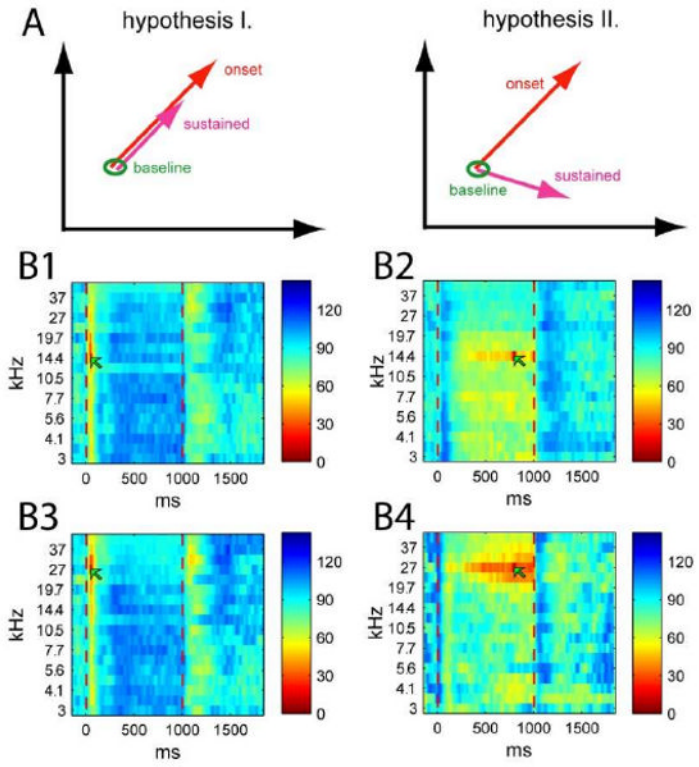

Figure 6. Population vector rotation

(**A**) Schematics of hypotheses tested in this figure. Hypothesis I: the population vector in the sustained period is a linearly scaled version of that at stimulus onset. Hypothesis II: both the magnitude and direction of the population vector changes. (**B1**) Pseudocolor plot showing the angle in degrees between the mean population firing rate vectors for all times and tone frequencies, and a reference vector produced by a 14.4 kHz tone during stimulus onset (indicated by the arrow). The reference vector is more similar to onset response vectors for other frequencies, than to sustained responses for the same tone. (**B2**) Similar analysis for a reference vector computed during the sustained response, here showing greater similarity to sustained responses of other stimuli, than to onset responses to the same stimulus. (**B3-4**) Same as B1-2, with 27 kHz tone response as reference. Adapted from Bartho et al (2009).

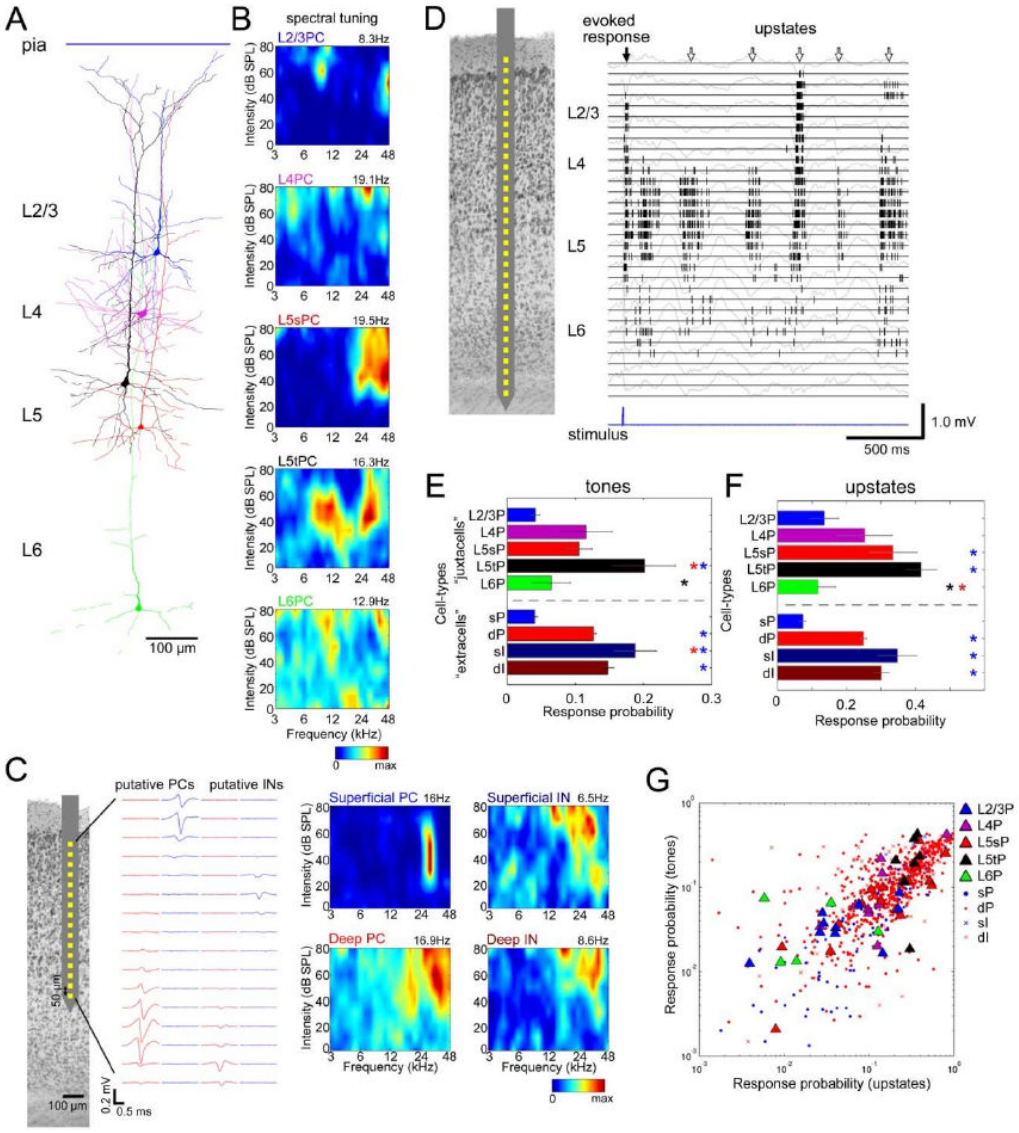

Figure 7. Cell-type dependent sparseness of population activity

(A) Examples of five juxtacellularly recorded pyramidal cells (PCs), digitally superimposed. **(B)** Spectral tuning of the neurons shown in (A). Each plot shows a pseudocolor representation of the cell's mean firing rate in a 50ms period following tone onsets, as a function of tone frequency and intensity. The number above each plot indicates maximum firing rate. L5sPC, L5 slender PC; L5tPC, L5 thick PC. **(C)** Tuning of four representative cells identified from silicon probe recordings. *Left*, schematic drawing of electrode, and average spike waveform profiles of a putative deep PC, superficial PC, deep interneuron(IN), and superficial IN. *Right*, spectral tuning of these cells. **(D)** *Left*, schematic drawing of recording by a 32-site linear electrode. *Right*, raster plot of multi-unit activity (MUA) for each channel, superimposed on local-field potentials (gray traces). **(E,F)** Sparseness of evoked and spontaneous activity was assessed using a “response probability” measure, for which smaller values indicate sparser firing. Bars above and below dotted line indicate cell-classes identified morphologically by juxtacellular recording (“juxtacells”), and silicon probe-recorded units putatively classified by spike waveform (“extracells”), respectively. Asterisks denote pairwise post-hoc lsd tests, indicating a significant difference

($p<0.05$) to the class corresponding to that color. Post-hoc comparisons were performed for juxtacells and extracells separately. sP, superficial PCs; dP, deep PCs; sI, superficial INs; dI, deep INs. Error bars indicate SE. **(G)** Sparseness is correlated between sensory responses and upstates. Each symbol shows the response probability of one cell to tone and click stimuli, with large symbols indicating juxtacells. Adapted from Sakata and Harris (2009).

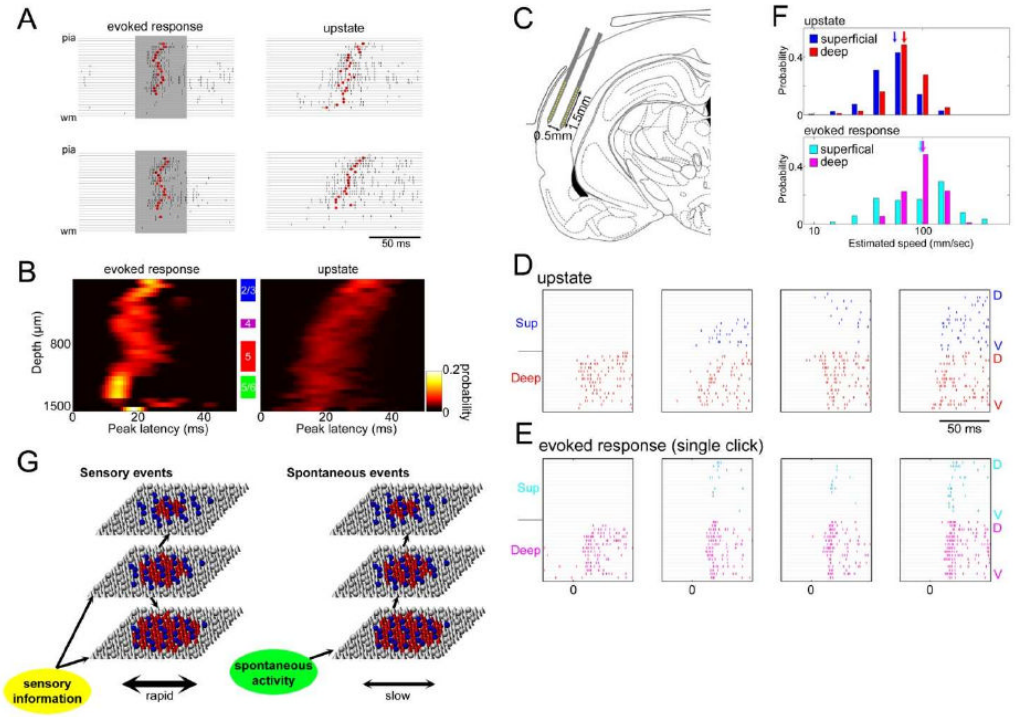

Figure 8. Difference in propagation of activity across cortical layers and columns

(A) Example laminar profiles of upstates and evoked responses. Rasters indicate MUA of all channels on a 32-site linear probe for individual upstates and evoked responses. Shaded periods indicate tone presentations. Red dots indicate "peak latency," computed as the median MUA spike time in a 50-ms window after event onset. **(B)** Laminar profiles of peak latency for tone-evoked responses (best frequency, 60-80 dB SPL) and upstates. The graphs show a pseudocolor histogram of the distribution of peak latency as a function of depth. **(C)** Two-shank multisite electrodes (2×16 linear probe) were inserted parallel to the layers of auditory cortex. A part of the drawing was replicated from (Paxinos & Watson 1997). **(D,E)** Examples of spatiotemporal patterns for upstates (**D**) and click-evoked responses (**E**). Each plot shows rasters of MUA on all recording sites, with superficial and deep shanks on top and bottom. The sites on each shank are arranged from dorsal (D) to ventral (V). **(F)** Distribution of propagation speeds for upstates (*top*) and evoked responses (*bottom*), estimated as the regression slope of median MUA time across recording sites. Arrows indicate the median, and the x-axis is log-scaled. Propagation speed was faster for evoked responses than for upstates in both layers (ANOVA with post hoc lsd test, $p<0.0001$). **(G)** Hypothesized flow of sensory-evoked and spontaneous activity through auditory cortical circuits. Each sheet represents a population of the corresponding layer, with cones and spheres representing PCs and INs, respectively. Colored symbols represent active neurons. Adapted from Sakata and Harris (2009)

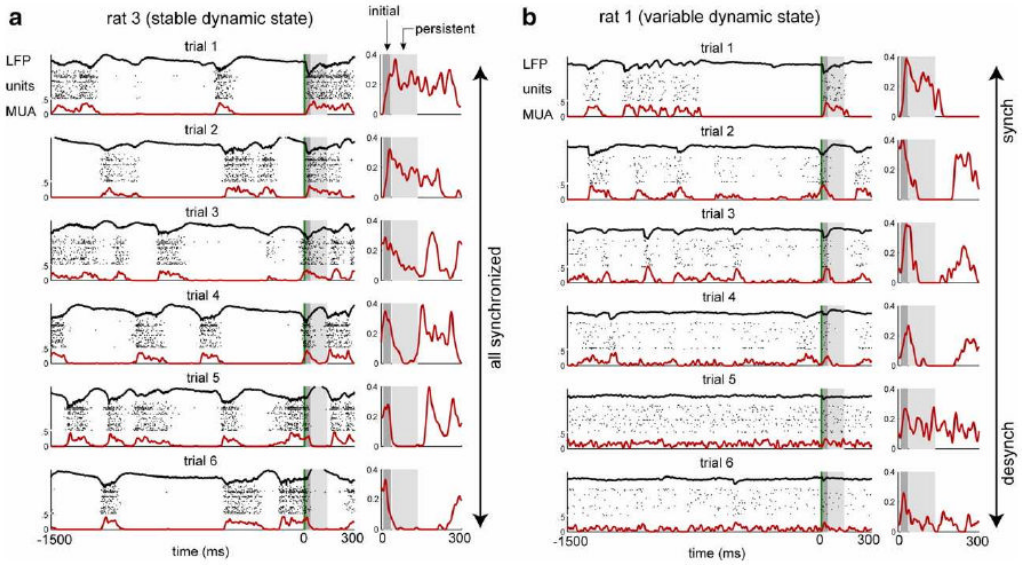

Figure 9. Trial-to-trial variability across a range of cortical states

(**A**) Six examples of population responses to click stimuli, from a rat that exhibited stable dynamic state throughout the recording. Vertical green lines denote stimuli (time 0); LFP (black trace), activity of simultaneously recorded single neurons (rasters) and smoothed multi-unit activity (MUA; red trace) all show a pattern of population activity characteristic of the synchronized state. Right column shows an expanded view of the smoothed MUA in the response period for each trial; gray shaded areas denote “initial” (10-35ms; dark gray shading) and “persistent” (40-135ms; light gray shading) response periods. The stimulus may arrive during a downstate (trials 1, 2), at the beginning of an upstate (trials 3, 4), or well into an upstate (trials 5, 6). While preceding activity does not have a clear effect on peak activity levels in the initial response period, the timing of the stimulus relative to up/down transitions appears to modulate activity in the persistent response period. (**B**) Same conventions as in (a); all data are selected from a different recording session that showed variable dynamic state. In the synchronized state (trials 1,2), persistent responses are anticorrelated with activity levels in the 200-300ms preceding the stimulus. In intermediate states (trials 3,4), the stimulus induces a large initial response followed by a transient downstate. In the most desynchronized states (trials 5,6), responses exhibit a small but reliable initial response followed by a return to baseline, with no discernible persistent response. Adapted from Curto et al (2009).

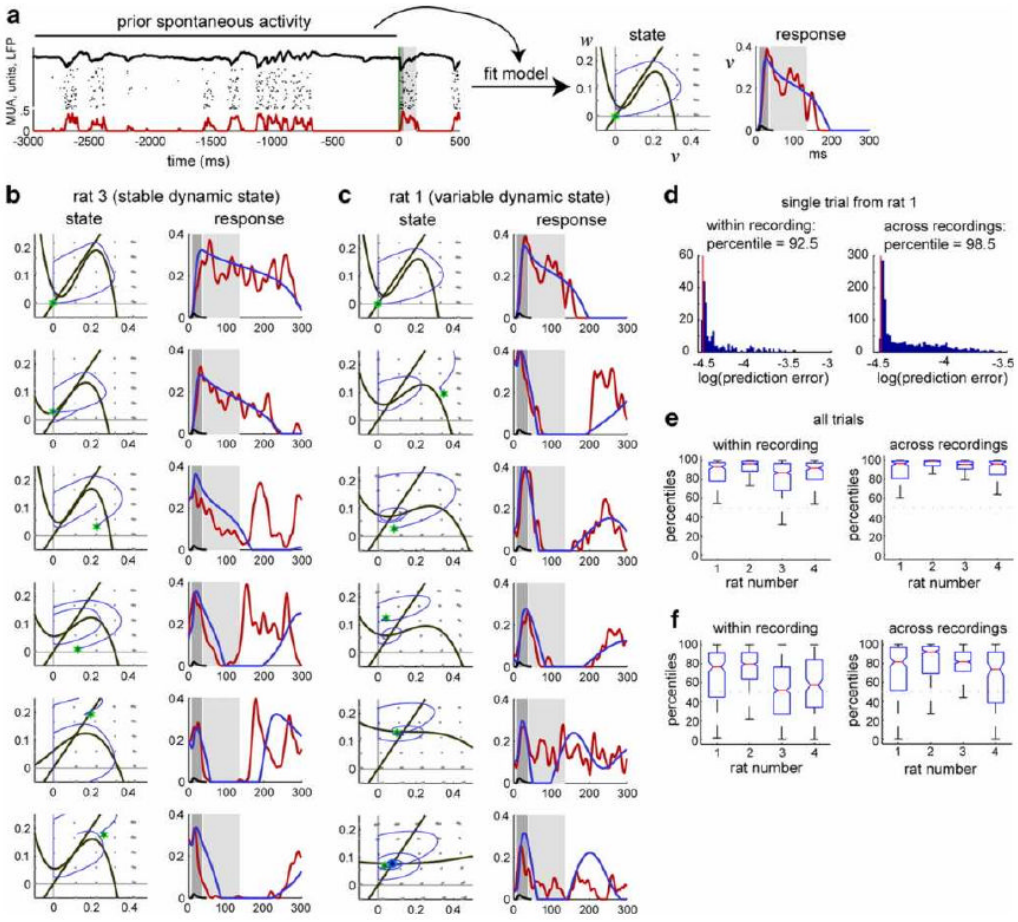

Figure 10. Stimulus-evoked responses can be predicted from models fit on prior spontaneous activity

(**A**) Methodology. 3s of spontaneous activity preceding the stimulus is used to fit the model parameters. The model-fit dynamic state (illustrated by the corresponding phase diagram), together with the activity state at the time of the stimulus (green star), is then used to simulate an evoked response (blue), shown superimposed on the true response (red). As in Figure 9, time 0 corresponds to presentation of click stimulus and shaded regions correspond to initial (dark gray) and persistent (light gray) response periods. (**B, C**) Estimated dynamic states and simulated responses for each trial displayed in Figure 9. (**D**) Histograms of prediction error for a single trial from rat 1 (red line), compared to predictions for the response on this trial made from states estimated for all other trials. Estimates from other trials, both within the same recording (left) and from other recordings (right), produced worse predictions. (**E**) Box plots of model fit percentiles for each trial, within and across recordings. Median percentiles (red) are in each case significantly above chance level (50%). (**F**) Same as in (e), but performance is compared using only dynamic states from other trials, keeping activity state at stimulus onset fixed. For recording sessions with high cortical state variability (1 and 2), percentiles were still high within and across recordings. For recording sessions with very stable dynamic state (3 and 4), percentiles were not significantly above chance within each recording, but remained high across recordings. Adapted from Curto et al (2009).